Establishing a Diode Laser Absorption Spectroscopy Laboratory in Quito, Ecuador

Master's Thesis
by
Christoffer Björkwall and Märta Cassel-Engquist

Lund Reports on Atomic Physics, LRAP 347
Department of Physics, Lund Institute of Technology
Lund, September 2005

Abstract

Diode laser absorption spectroscopy has many useful applications and has the advantage that the equipment in most cases is small, cheap, and easy to handle. A laboratory in this field of research and education has been established at the Department of Physics at Escuela Politécnica Nacional in Quito, Ecuador as a Master's project.

The laboratory equipment was sponsored by the International Science Programme in Uppsala, Sweden. It includes two systems, one for studying rubidium absorption and one utilizing the GASMAS technique; GAs in Scattering Media Absorption Spectroscopy. This technique has been used for in-situ studies of free molecular oxygen embedded inside scattering media, properties unique for this technique. The GASMAS technique was introduced in 2001 at the Division of Atomic Physics, Lund Institute of Technology, Sweden.

The scope of the project was to prepare the equipment for transportation, transfer technology and knowledge about it on site in Quito, assemble the set-ups, and finally make experiments on topics of high potential for Ecuador. Measurements on fruits, polystyrene foam, volcanic rocks, and balsa wood were performed.

Contents

Chapter 1

Introduction

Before the beginning of this project there were only two laboratories in the world with GASMAS set-ups; **GA**s in **S**cattering **M**edia **A**bsorption **S**pectroscopy [1]. The original set-up is located at the Division of Atomic Physics at Lund Institute of Technology (LTH) in Lund, Sweden. Another one, donated by International Science Programme and assembled by the Lund diode laser spectroscopy group at LTH, is located at the University of Zimbabwe in Harare, Zimbabwe. As a result of this Master's project, there is now also one at the Department of Physics, at Escuela Politécnica Nacional (EPN) in Quito, Ecuador. This report will describe the full process of preparing, mounting, and testing a diode laser spectroscopy laboratory, containing both a GASMAS set-up and an absorption set-up for rubidium gas, from its beginning in Lund to its conclusion in Quito.

1.1 Background

In 1961 an organization named International Science Programme, ISP, was founded at the Uppsala University, Sweden, in order to improve research in developing countries in mathematical, physical, and chemical sciences. Its philosophy is to help build up research on site in the countries in long-term cooperations. After an application from Prof. Edy Ayala at EPN, the organization decided in 2004 to finance a laboratory for absorption spectroscopy research at EPN. The Division of Atomic Physics at LTH was made responsible for ordering the equipment. The equipment was bought, and parts were manufactured in the mechanical workshop at LTH.

MSc. Gabriel Somesfalean, who had pursued the Harare Project including a visit for integration at University of Zimbabwe, also did these arrangements for the project in Quito. Although, due to his upcoming PhD dissertation, the project could not be completed.

In discussions with Prof. Sune Svanberg at the Division of Atomic Physics at LTH, a Master's project for the authors was formed with the aim of finalizing the original Quito project. With the different study background of the authors, Electrical Engineering and Engineering Physics, useful knowledge could be brought from a wide range to the project. MSc. Linda Persson, graduate student in the Lund diode laser spectroscopy group was involved in the project. She functioned as a mentor, providing very valuable guidance and inspiration to the project. She also made a visit to the Quito site to contribute in the project.

With the completion of the present project and with the inclusion of an already existing diode laser set-up for laser-induced fluorescence spectroscopy in Quito, being the result of a previous development project [2], diode laser spectroscopy is now firmly established in Ecuador.

1.2 Purpose

The purpose of the project was to establish a diode laser research and teaching laboratory at EPN for diode laser absorption spectroscopy. In the future, this laboratory will allow the possibility to perform research and have a good environment for education in the area of absorption spectroscopy.

Our task was to prepare the equipment in Lund before transport, assemble the experimental stations on site in Ecuador, and initiate experimental studies. It became clear that there was also a need to perform informational activities about the equipment and its applications, for the students and possible cooperation partners, on site.

The purpose of this report is not only to leave a detailed report about the Master's project, but also to produce a good source of information for the people who will continue the work on the absorption spectroscopy set-up at EPN.

1.3 Goal

The goal of the project was to leave a well functioning absorption spectroscopy laboratory, both for education and research, together with the know-how about it for future researchers and supervisors. Another goal was to investigate a research field of interest to the country of Ecuador, possible to be investigated with the GASMAS technique, and to pursue initial experimental studies with the equipment.

1.4 Achievements

After checking and preparing in Lund, the equipment was successfully delivered to EPN, after about a two months delay at the customs of Ecuador. This time of delay was partially spent by performing information activities such as making a poster, holding a presentation, and making connections with possible research partners. Once the equipment arrived, it was assembled and optimized as planned. During this part a local Diploma student, Ms. Yolanda Angulo, was taught about the systems and was step-by-step involved in the mounting and investigation processes.

Together with our local supervisors at EPN, Prof. Edy Ayala and Dr. César Costa ,different investigations were planned and performed. Measurements were made on fruits, balsa wood, volcanic rocks, and polystyrene foam with promising results.

Additionally, an introductory laboratory exercise was created for GASMAS and applied. A laboratory exercise for the rubidium set-up was also translated from a corresponding activity used at LTH. A program was developed in LabVIEW making it possible to perform automated and unattended long-time measurements. As a help for future researchers on GASMAS at EPN, a user manual was made. In order to make information about the systems and laboratory exercise instructions easily accessible, a website was constructed and uploaded on the EPN website.

1.5 Outline

This report contains a theory chapter, Ch. 2, that treats the basic component of diode laser absorption spectroscopy; interaction between light and matter,

diode lasers, and modulation techniques. The theory chapter ends with a description of the GASMAS system and method. Ch. 3 describes the different parts of the equipment. The other chapters are placed in chronological order as they followed in the project; Ch. 4 describes the preparations in Sweden, Ch. 5 the informational activities performed when the authors arrived to Quito, Ch. 6 the assembly and Ch. 7 the experimental part. The report ends with a summary and a conclusion, Ch. 8, including a brief discussion of future work.

Chapter 2

Theory

To understand absorption spectroscopy, knowledge of how light interacts with matter is needed. Useful tools in absorption spectroscopy contexts are the diode lasers. Many times in absorption spectroscopy the signals obtained are very small, and a way to increase the sensitivity is to use modulation techniques, which for example the GASMAS technique uses.

2.1 Light propagation in matter

When an incident beam of light strikes a material, different interactions take place. In general, there are three possibilities: the light can be *reflected*, *absorbed* and/or *scattered*, see Fig. 2.1. Depending on the specific material, one or two of these actions dominate over the other.

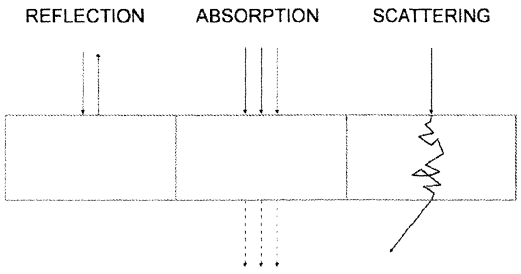

Figure 2.1: *The three possible interactions between light and matter; reflection, absorption, and scattering.*

2.1.1 Reflection

A light beam that hits a surface between two media will be partially reflected, due to the change in refractive indices, n. The *reflectance*, R, is calculated as

$$R = \left(\frac{n_2 - n_1}{n_2 + n_1}\right)^2, \tag{2.1}$$

where n_1 is the refraction index of the medium where the light beam travels from and n_2 is the refraction index of the medium being hit by the light beam. The reflectance is the fraction of the incident light being reflected [3].

2.1.2 Absorption

Atoms and molecules absorb energy at certain frequencies or wavelengths. This is an effect of their electronic shell structure and the vibrational and rotational energy levels. If the photon energy, i.e. its frequency or wavelength, is suitable to the atom or molecule, it may absorb the energy and get excited. Every atom and molecule has a unique set of absorption lines, i.e. a "fingerprint". This makes it possible to identify for example a gas with absorption analysis [4, 5].

When the absorption is much greater than the scattering, it is theoretically described by the *Beer-Lambert law*

$$I(\nu, x) = I_0(\nu)e^{-\sigma(\nu)c \cdot x}. \tag{2.2}$$

It states that the intensity of the incident light, I_0, is attenuated exponentially through an absorbing material, see Fig. 2.2. The cross section of absorption, σ, is the probability of absorption with a unit of area per molecule or atom. The concentration of absorbing molecules or atoms is c, and x is the length traveled through the medium. When no scattering occurs, this length is the same as the physical thickness of the sample. The cross section is frequency dependent, matching the energy level structure [4, 5].

A derived property $a(\nu)$ is called the *absorbance*. It is defined as

$$a = \sigma(\nu_0)c \cdot x, \tag{2.3}$$

where $\sigma(\nu_0)$ is the absorption cross section at the frequency ν_0, the center of the line [5]. It is usually absorbance that is measured in absorption spectroscopy experiments.

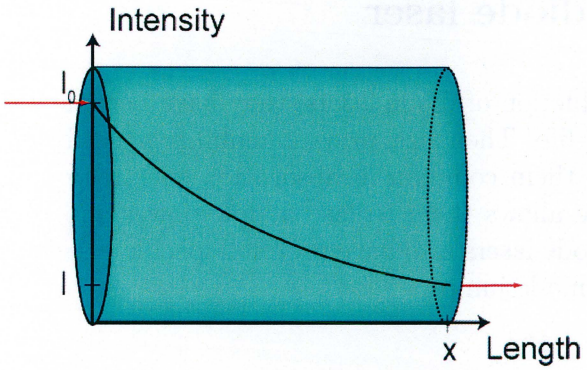

Figure 2.2: *The absorption of a beam with the intensity I_0, according to the Beer-Lambert law.*

All materials absorb differently depending on the physical state and composition. Solids, liquids, and gases all have different absorbing features. Gases have much sharper absorption lines than solids or liquids, for which the atoms or molecules undergo complex interactions [1].

2.1.3 Scattering

Scattering occurs when an incident beam interacts with a particle and the reemission of the energy, or parts of it, is in many directions. This effect is a result of the emission of the forced oscillating electric charges, from the alternating electrical fields [3]. The scattering process results in the *path length*, the distance the photons travel, being different from the thickness of the sample, see *Scattering* in Fig. 2.1.

There are different scattering processes and which one of them that occurs depends on the material and the wavelength of the incident light beam. If the particles causing the effect are small compared to the wavelength, it is called either *Rayleigh* or *Raman scattering*. If the particles are large in comparison with the wavelength, it is called *Mie scattering*. The Rayleigh and Mie scattering are elastic effects, the energy is conserved in the processes. The Raman scattering is inelastic, meaning the energy is changed in the process, and thus the wavelength is shifted [3, 4].

2.2 The diode laser

Since the introduction of diode lasers, they have become a common component in our daily life. Their size, price, and ability to easily tune in wavelength have also made them common in absorption spectroscopy. Their semiconductor structure allows them to lase at low power and room temperature. However, the diode lasers also have product-specific disadvantages like beam divergence and mode jumps.

2.2.1 History

The first version of the diode laser was developed simultaneously in 1962 by four different and independent science groups. The first diode lasers developed were *homojunction-based* units and had to operate at temperatures of only a few Kelvin. Later during the same decade, the *heterojunction-based* lasers were discovered and made more or less the homojunction-based lasers obsolete. The heterojunction lasers function at room temperature, which opened possibilities for many new applications [7]. During the 1980's this laser type experienced a rapid increase in commercial use, particularly regarding telecommunications [8]. One application, among many, that became more available because of this was laser spectroscopy [4].

2.2.2 Advantages

Diode lasers are the most commonly used lasers in the world today. It is possible to find them in products such as CD players, bar-code readers and within optical communication systems [8]. The wide use of diode lasers has made them mass produced and thus relatively cheap, with prices ranging from $1 a piece [9]. Although, since they are normally produced for commercial application purposes and not for research experiments, they might not have exactly the wavelength or features sought for. They also have a property referred to as mode jumps, see Sect. 2.2.4, which limits the wavelengths available [8]. There are custom made diode lasers on the market, guaranteed not to have mode jumps. However, these Distributed Feedback lasers, or DFB lasers, are more expensive [10]. By testing several mass produced lasers, it is possible to find lasers suitable for research, at a low price.

Another advantage of diode lasers, in comparison to other laser types, is their size. The diode lasers, including shielding and connectors, are normally

only the size of a green pea, see Fig. 2.3. This enables possibilities to build compact equipment.

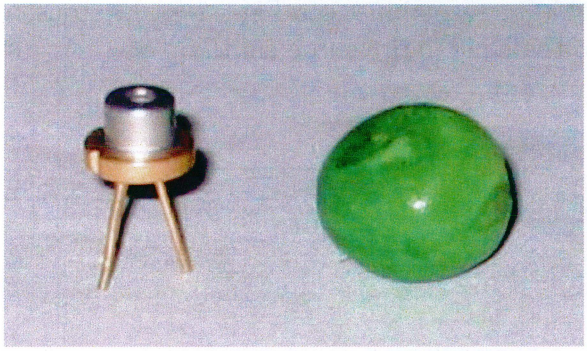

Figure 2.3: *A diode laser and a green pea.*

Other attractive features of diode lasers are their energy efficiency and easy operation. The major advantage of diode lasers for spectroscopic purposes, however, is their ability to be tuned in wavelength. The ability to scan the wavelengths around an absorption line is a key feature for absorption spectroscopy [4].

2.2.3 Basic principles

Diode lasers, or semiconductor lasers, are produced using advanced material processing techniques, as a compound of different materials. The materials used depend on which wavelength the laser is intended for. It is today possible to reach wavelengths between 0.4 to 29 μm. The majority of the diode lasers are made of doped materials from group III (e.g. Al, Ga, In) and group V (e.g. N, P, As, Sb) in the periodic system. Diode lasers made from these materials emit light in the wavelength range 600-1600 nm [7]. There are two general types of diode lasers; homojunction lasers and heterojunction lasers. Homojunction lasers has a more simple construction than heterojunction lasers and will be described as a mean to understand the function of diode lasers.

Homojunction lasers

A homojunction diode laser is created by joining semiconducting materials, doped in different ways. One part is *n doped*, has an excess of electrons,

and the other one is *p doped* which means it has a lack of electrons, so called *holes*. When a voltage is applied over the semiconducting material the electrons from the conduction band and holes from the valence band will diffuse and be able to recombine, see Fig. 2.4. Photons, with the energy corresponding to the band gap, will be emitted [7].

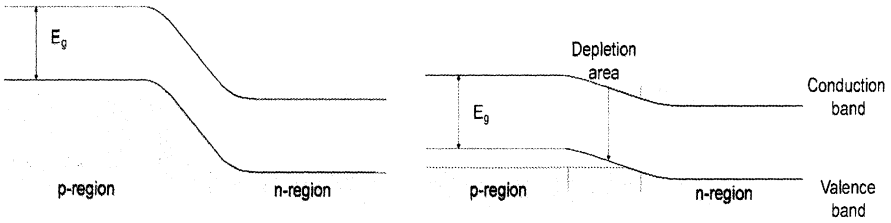

Figure 2.4: *A homojunction laser with valence and conduction bands. The left figure shows the bands without a bias voltage and the right shows the bands with a bias voltage being applied over the laser.*

The homojunction lasers have a major drawback; they cannot work at room temperature. This is due to the large thickness of the active medium and losses from absorption in the junction. This results in the need of a very high current at room temperature for the diode to be able to lase [7].

Heterojunction lasers

The problem the homojunction lasers have with the operation temperature is solved for heterojunction lasers. They have an active layer, also a semiconductor, sandwiched between the two semiconductor layers with higher band gap energies, see Fig. 2.5. Since the photons created in the active layer do not have the energy corresponding to the surrounding band gaps, the photons will not be absorbed. This allows the laser to operate at room temperature [7].

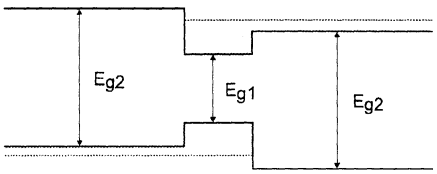

Figure 2.5: *The band gap structure of a heterojunction laser showing the active layer in the middle, with the energy gap E_{g1}. The surrounding band gaps, E_{g2}, have a higher energy gap than the active layer.*

Laser production

First, the light will be spontaneously emitted and amplified with the help of a gain medium in an optical resonator, a so called cavity. The cavity is formed by having a reflectance of about 30 % on the cleaved faces of the semiconducting material. The spontaneously emitted photons being mirrored will cause *stimulated emission*, emitting photons with the same phase and wavelength, and if population inversion is provided, the laser will start to lase [7].

The output power of the diode laser rapidly escalates once a threshold current, I_{th} has been reached, see Fig. 2.6. Exceeding a certain level of output power, will cause the laser beam to irreversibly destroy the semiconductor facets, and thus the entire laser [7].

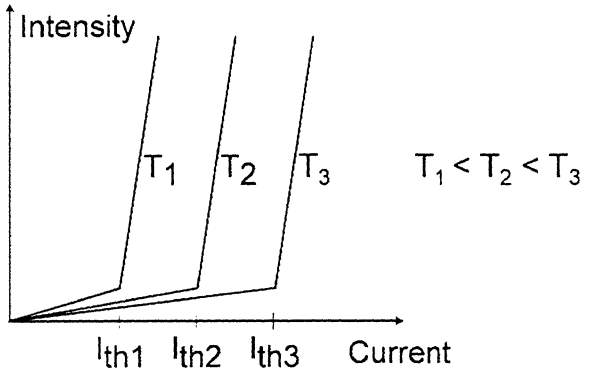

Figure 2.6: *The output power as a function of the injection current for different temperatures, T. The diode laser starts to lase at a threshold current, I_{th}.*

2.2.4 Optical properties

There are some disadvantages with diode lasers; for example the output beams are astigmatic, assymetric, and divergent. The astigmatism is a result of the fact that the refractive index has a directional dependence. The assymetrical and divergent properties are due to the assymetrical shape of the diode laser (normally rectangular 1 μm $\times$ 3 μm in the active layer). This results in a 30-40° $\times$ 10-20° divergence. The beam, however, resembles a Gaussian profile minimizing the problem. The problem with divergence of the laser beam can rather easily be handled with a collimating lens [8].

2.2.5 Mode jumps

The major drawback of diode lasers is that they tend to *mode jump*. These discrete jumps in wavelengths, see Fig. 2.7, are due to a shift in gain curve. Mode jumps constitute a hazzle in absorption spectroscopy since they limit the possibility to tune the wavelength. They severely limit the wavelengths possible to reach with a particular diode laser [8].

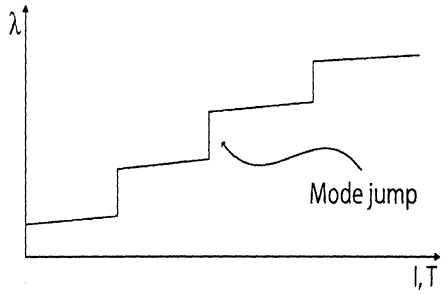

Figure 2.7: *Mode jumps making discrete jumps in wavelengths when the current or the temperature to the diode laser is changed.*

2.2.6 Tunability

The great advantages of diode lasers for spectroscopy overshadow the disadvantages. Diode lasers have high spectral purity, high wavelength stability, great modulation capabilities, and most important of all; tunability. The possibility to tune the wavelength of the laser is what makes diode laser spectroscopy possible and simple [8].

The wavelength output from a diode laser, is dependent on both temperature and injection current. There is a temperature dependency of the band gap and by varying the current, the gain curve and thus the wavelength is changed. The refractive index of the band gap is also temperature dependent and can be altered by directly changing the temperature of the diode. Thus, it is possible to use both temperature and injection current as tools to change the output wavelength of a diode laser. The methods differ regarding the wavelength shift produced. A band gap temperature shift makes a difference of about 0.25 nm/°C and a change in refractive index of about 0.06 nm/°C [8]. The relation between current and wavelength is in the order of 10^{-3} nm/mA [11]. Practically, this means that temperature is used for coarse tuning and the injection current is used for fine tuning of the wavelength.

However, there are problems involved in tuning diode lasers. The standing wave in the laser cavity determines the wavelength sent out from the diode laser. In order to have a well-defined wavelength, the diode laser has to operate in a *single mode*. Single-mode operation means that there is only one standing wave in the cavity and thus only one wavelength being emitted. The opposite condition, *multi-mode operation*, occurs when there are more than one standing wave simultaneously in the cavity. This is due to the frequency separation between the modes being smaller than the width of the gain profile of the laser [7]. A multi-mode behavior results in more than one wavelength competing in the output.

2.3 Absorption spectroscopy

With absorption spectroscopy it is possible to investigate a sample quantitatively and qualitatively. Every material has its own fingerprint created by the energy levels in the atom or the molecule. From the results of absorption spectroscopy the concentration, temperature, and pressure of a gaseous sample can be quantified [4].

An absorption spectroscopy set-up consists of three main parts; a *light source*, an *absorbing sample*, and a *detector*. The light is sent through the sample and the output light is detected and measured as shown in Fig. 2.8.

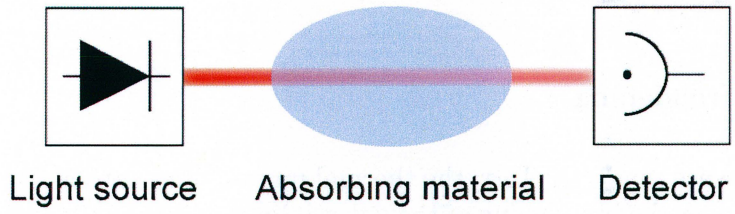

Figure 2.8: *Figure showing the three main parts of an absorption spectroscopy set-up for gas samples; a laser source, a sample absorbing the laser beam, and a detector.*

When diode lasers are used in absorption spectroscopy it is referred to as TDLAS, Tunable Diode Laser Absorption Spectroscopy. By letting the injection current to the diode laser have a saw-tooth shape, it is possible to repetively sweep over the absorption line and detect it in real time. The wavelength in the diode laser needs to be narrow and operate in single mode to be able to detect the absorption lines. Lasers have a finite line width, and

it is of great importance that this width is smaller than the absorption line, to detect it [5].

2.3.1 Line shapes

An absorption line always has a finite width. How wide it is and the shape of the line depends on the sample temperature, pressure, and the surrounding materials. A way to characterize the broadening of the line is through stating the *Full Width at Half Maximum*, FWHM [4].

Natural line width

Every absorption line has a *natural line width*, $\Delta\nu_n$. This is related to the lifetime of the state as indicated by Heisenberg's uncertainty principle. The principle states that with an uncertainty in time, Δt, there is always an uncertainty in energy, ΔE, and thus frequency [4]

$$\Delta E \cdot \Delta t \geq \frac{\hbar}{2}. \tag{2.4}$$

The natural line width is under standard conditions only at an order of 0.1-100 MHz [5].

Doppler broadening

At low pressure, under 10 Torr, the thermal motion of the atoms or molecules dominates over the broadening of the natural lines. This is called the *Doppler broadening*, $\Delta\nu_D$, and is dependent of the temperature, T, and molecular mass, M, of the sample

$$\Delta\nu_D = const \cdot \nu_0 \sqrt{\frac{T}{M}}. \tag{2.5}$$

The Doppler broadened line has a Gaussian line shape [4]. This broadening is about 1 GHz in the visible region and thus strongly dominates over the natural line width.

Pressure broadening

Collision effects dominate over other broadening effects at atmospheric pressure, producing a Lorentzian shape on the absorption line profile. At standard conditions, atmospheric pressure and ambient temperature, the pressure broadening is about 3 GHz and thus dominates over the Doppler broadening and the natural line width [5]. The collisions shorten the lifetime of the excited state because of deexcitation [4]. The *pressure broadening*, $\Delta\nu_L$, is dependent of the pressure according to

$$\Delta\nu_L = \sum \gamma_i \cdot p_i, \tag{2.6}$$

where p_i is the partial pressure and γ_i is the partial pressure broadening coefficient [5].

At intermediate pressures, 10 - 100 Torr, the resulting profile is a convolution of a Gaussian and a Lorentzian profile. This is called a *Voigt* profile and has to be computed numerically [5].

2.3.2 Analysis

The properties which can be achieved through absorption spectroscopy are the concentration, temperature, and pressure of the sample. The absorbance can be calculated by measuring I and I_0, see Fig. 2.9, and using Eqs. 2.2 and 2.3. To be able to determine the concentration, the optical path length and the absorption coefficient need to be known. In samples where scattering is not an issue, the optical path length is the same as the geometrical length of the sample. It is also possible to determine the concentration by comparing the signal with a signal obtained from a calibration sample, with a known concentration.

2.4 Modulation

Modulation techniques are used to enhance the detection of small absorption signals. Frequently, phase-sensitive detection is accomplished by the use of a lock-in amplifier.

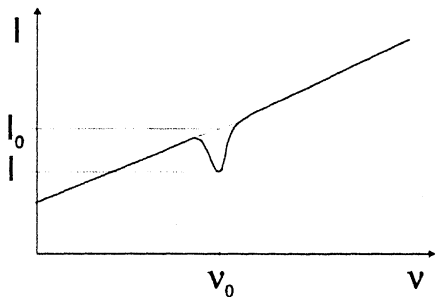

Figure 2.9: *A schematic showing a sweep in frequency over an absorption line at ν_0. I is the recorded intensity at ν_0 and I_0 is the intensity if no absorption would take place.*

2.4.1 Advantages

When a diode laser scans the wavelength over an absorption line with a ramped signal, a *direct signal* from the detector is obtained. In some cases, absorption spectroscopy on rubidium for example, it is possible to observe the absorption in the direct signal, e.g. see Fig. 2.9. In other applications the absorption signal is smaller than the surrounding noise. To extract these small signals from the background noise, modulation techniques together with a lock-in amplifier can be used.

2.4.2 Basic principles

Modulation means that a high-frequency sinusoidal signal is added to a carrier signal, e.g. the ramp that scans over an absorption line, see Fig. 2.10. The modulation frequency is also sent as a reference to a frequency- and phase-sensitive lock-in amplifier. The output signal from the detector, is filtered by the lock-in amplifier using the reference frequency, and analyzed. Through modulation, the signal is moved to a detection band at higher frequencies, where the noise level is lower [13].

A noise getting attenuated at higher frequency is the flicker noise, also known as $1/f$-noise since it is approximately proportional to the inverse frequency of the signal. In an electronical set-up, this noise stems from the resistors [14].

Modulation with the use of a lock-in amplifier could be explained as sitting in a noisy café in Quito with Spanish-speaking people around you. If someone

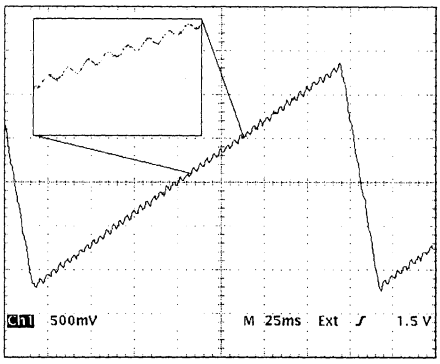

Figure 2.10: *A ramp, i.e. a direct signal, with an arbitrary superpositioned modulation frequency including a zoom-in on the modulation.*

talks Swedish a couple of tables away, you can probably hear that, through the noise, if you are a Swedish native speaker. Your brain (the lock-in amplifier) singles out the characteristics (the signal at the specific modulation frequency), the Swedish language, and the information is retrieved.

Using modulation in absorption spectroscopy is also referred to as *derivative spectroscopy*, since the modulation signal gets the form of a derivative of a certain order, if the modulation is small in amplitude [15, 16]. In Fig. 2.11 the direct signal is shown for an absorption signal and a mode jump together with their resulting lock-in signal if the second harmonic output is studied. The lock-in signals are then proportional to the second derivative of the direct signals [16].

2.4.3 Lock-in amplifier

The key instrument in modulation techniques is the lock-in amplifier. This instrument uses a technique called *phase-sensitive detection* to detect AC signals, as small as nanovolt, with a very good signal-to-noise ratio.

The lock-in amplifier uses an external reference frequency to modulate the experimental system ω_R, and to create an internal signal ω_L, thus $\omega_L = \omega_R$.

The lock-in amplifier creates an internal signal, $V_L sin(\omega_L t + \varphi_L)$, from the input reference signal from the modulation generator. The input signal to the lock-in amplifier, obtained from the modulated experimental system, $V_{sig} sin(\omega_R t + \varphi_R)$, is amplified with a pre-amplifier on the lock-in amplifier. The two signals are multiplied by the lock-in amplifier leading to a

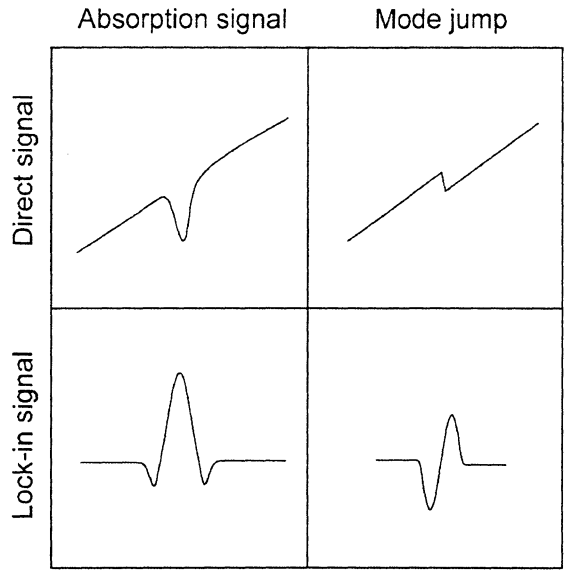

Figure 2.11: *Schematic theoretical comparison between an absorption signal and a mode jump in the direct signal, together with their corresponding lock-in signals. The lock-in signals correspond to the second derivative of the direct signal.*

signal containing two AC signals, one with the added frequencies, $\omega_R + \omega_L$, and one with the subtracted frequencies, $\omega_R - \omega_L$.

$$\begin{aligned} V_{PSD} &= V_{sig} sin(\omega_R t + \varphi_R) \cdot V_L sin(\omega_L t + \varphi_L) \\ &= \frac{1}{2} V_{sig} V_L cos((\omega_R - \omega_L)t + (\varphi_R - \varphi_L)) \\ &\quad -\frac{1}{2} V_{sig} V_L cos((\omega_R + \omega_L)t + (\varphi_R + \varphi_L)) \end{aligned}$$

The multiplied signal, V_{PSD}, is filtered with a low-pass filter, leading to the AC signal with the added frequencies being eliminated. The remaining signal will be a DC signal, since $\omega_R - \omega_L$.

$$\begin{aligned} V_{PSD} &= \frac{1}{2} V_{sig} V_L cos((\omega_R - \omega_L)t + \varphi_R - \varphi_L) \\ &= \frac{1}{2} V_{sig} V_L cos(\varphi_R - \varphi_L) \\ V_{PSD} &\propto V_{sig} cos(\varphi_R - \varphi_L) \end{aligned}$$

This DC signal, $V_{sig}cos(\varphi_R - \varphi_L)$, can be adjusted to its maximum amplitude by changing the phase to: $\varphi_R = \varphi_L$. The DC signal, V_{PSD}, is proportional to the sought signal and denoted in this report as the *lock-in signal.*

There are three important properties of the lock-in amplifier when optimizing the signals; the phase, the sensitivity setting, and the time constant. The phase setting changes φ_L and thus also the amplitude of the obtained lock-in signal. The sensitivity setting changes the amplification of the pre-amplifier. The time constant refers to the time constant of the slope of the low-pass filter.

2.5 GASMAS

GASMAS, GAs in Scattering Media Absorption Spectroscopy, has common features with other types of gas absorption spectroscopy. It uses the three basic modules: the light source, the absorbing sample and the detector. What makes GASMAS unique is that it permits in-situ measurements of free gas inside a scattering solid or liquid. The GASMAS method can also give information about the pressure, temperature, internal structure, and diffusion characteristics of the investigated material [12]. The technique has, since its first appearance in 2001, been used to investigate a wide range of applications and subjects such as, polystyrene foam [12], gas exchange in fruits [17, 18], wood [6], packaging plastics [18], and diagnostic measurements on human sinuses [19].

2.5.1 Basic principles

In the GASMAS set-up the light from a diode laser, with a sharp spectral output, is sent into a scattering medium through an optical fiber, see Fig. 2.12. The light is scattered in the sample and the pores of the target gas absorb the light at its specific wavelength. This results in a signature in the output signal. This signal is detected with a photomultiplier tube, PMT, whose output signal is analyzed with modulation techniques. For GASMAS, two different measurement geometries are possible; *transmission* and *reflection* through backscattering [1, 18].

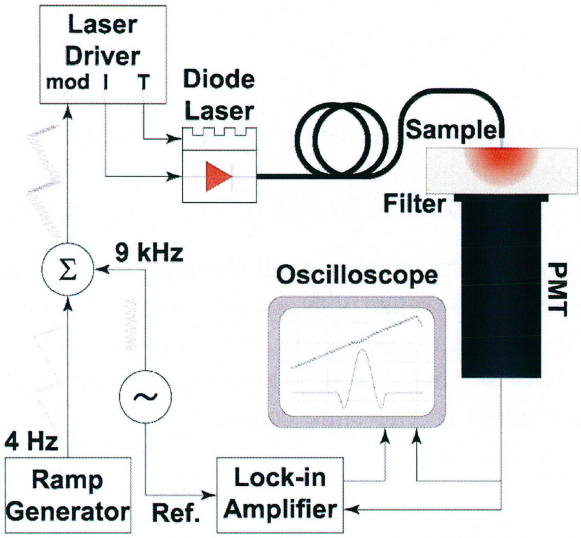

Figure 2.12: *Schematic picture of the GASMAS set-up.*

What enables the GASMAS method to sort out the absorption line from the free gas embedded in the scattering material, is the line characteristic. Gases have many times more narrow absorption lines, typically 10^4 times, than liquids or solids [6]. Thus, the narrow absorption gas line occurs in a background of a broad absorption feature that comes from the scattering material. Hence, it is possible to assume that these background properties are constant over the range the wavelength is tuned [12].

Due to the scattering, the path length of the photons is not the same as the thickness of the sample. This results in a more difficult approach to the Beer-Lambert law. There are ways of estimating the real distance the light has traveled. For this purpose, spatially resolved, time-resolved, or frequency-domain methods have been introduced. Then, by analyzing the scattering and absorption properties and using the Beer-Lambert law, the distance traveled by the average photon, can be calculated [1]. In some applications, it is not necessary to know this. In these cases it is enough to introduce a unit called equivalent mean path length, L_{eq}, as a relative measure of the concentration of gas inside the sample, see Sect. 2.5.3. This unit, however, also depends on the scattering properties of the sample [1].

For the modulation techniques, in GASMAS, it is convenient to use the second derivative of the signal due to the fact that the second derivative is not sensitive to the general slope of the direct signal. The GASMAS technique uses a modulation frequency in the kilohertz range, so called *wavelength*

modulation spectroscopy, since the frequencies are much smaller than the half width of the absorption line [13].

So far, GASMAS has only been used studying molecular oxygen embedded in scattering materials. The narrow absorption lines studied in molecular oxygen belong to the so called A band, see Fig. 2.13, at wavelengths around 760 nm. The absorption is due to transitions between vibrational and rotational states [5]. In theory, the only thing that needs to be changed to study another gas is the wavelength, hence the laser [6]. The detector might also have to be changed to be sensitive in the specific wavelength range.

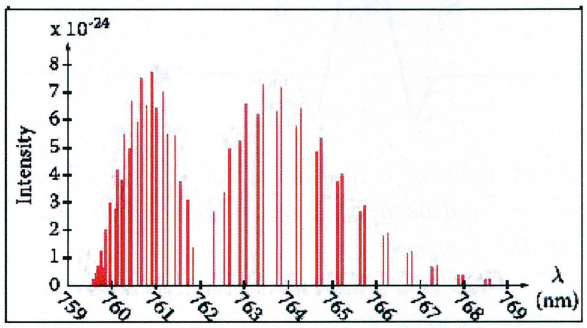

Figure 2.13: *The narrow absorption lines belonging to the A band of molecular oxygen [20].*

2.5.2 Normalization

When dealing with absorption spectroscopy it is of great importance to normalize the signals to be able to compare results. In GASMAS, normalization is calculated by taking the height of the lock-in signal divided by the interpolated DC intensity of the direct signal at the location of the absorption signature, see Fig. 2.14 and Eqs. 2.7 and 2.8. The normalized signal is referred to as the *GASMAS signal*, and denoted *GMS* [15].

$$S_{2f} = \frac{S_1 + S_2}{2} \tag{2.7}$$

$$GMS = \frac{S_{2f}}{S_{dir}} \tag{2.8}$$

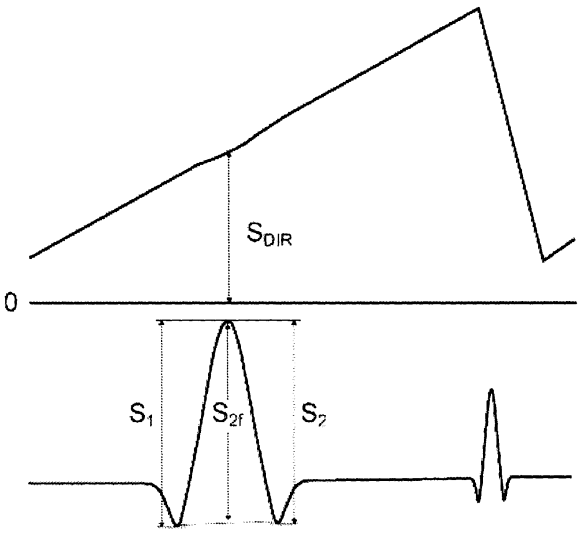

Figure 2.14: *An illustration of a theoretical direct signal and a lock-in signal as they appear on the oscilloscope screen. The definitions used for normalization are given in the figure.*

2.5.3 Standard addition

In GASMAS, the *standard-addition* method is introduced to determine an equivalent mean path length. The method is well known in physical chemistry and it relates the absorption signal to that of absorption in free air. The basis of this calibration technique is that a linear relationship between the absorption signal and the oxygen concentration is expected since the absorption signal is only a few percent of the signal.

An *equivalent mean path length*, L_{eq}, can be extrapolated by letting the laser light travel a known distance through a well-characterized oxygen-rich medium, such as normal air, and determining the increase in absorption signal, see Fig. 2.15. For a scattering sample, this would correspond to the distance the light would have to travel through air to obtain the same signal. For this reason the equivalent mean path length can be longer, or shorter, than the thickness of the measured sample [1]. The reason for using the standard-addition method and the equivalent mean path length unit is to transfer the rather abstract oxygen absorption into a tangible unit.

The equivalent mean path length depends on both the concentration of molecular oxygen and the scattering coefficient of the sample. In a highly scattering sample, the light will travel a longer distance along more compli-

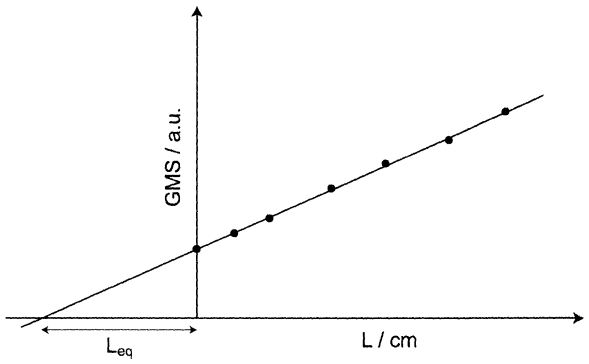

Figure 2.15: *Several standard addition measurements giving the equivalent mean path length through an extrapolated line.*

cated pathways. Hence, there will be a larger probability to find molecular oxygen. The real concentration of molecular oxygen in the sample, c_{sm}, can then be related to the concentration in free air, c_{air}, by using L_{eq} according to

$$c_{air}L_{eq} = c_{sm}L_{sm}, \tag{2.9}$$

where L_{sm} is the actual optical path length traveled by the light inside the sample [12].

2.5.4 Restrictions

A very important limitation one has to deal with when performing gas absorption measurements in the general case, is the absorption of other compounds. The interferences depend on the sample type and the spectral region being analyzed. Among the most important interferences is the ubiquitous water vapor. Water is widely distributed in all types of biological tissue and strongly absorbs light for wavelengths larger than 1400 nm [1]. Hemoglobin absorption practically eliminates all light transmission for wavelengths shorter than 600 nm. The oxygen absorption lines that GASMAS uses are between these wavelengths, around 760 nm, making it possible for the light to penetrate human tissue without substantial absorption by these compounds, see Fig. 2.16. The wavelength range between 600 nm and 1400 nm is called the tissue optical window.

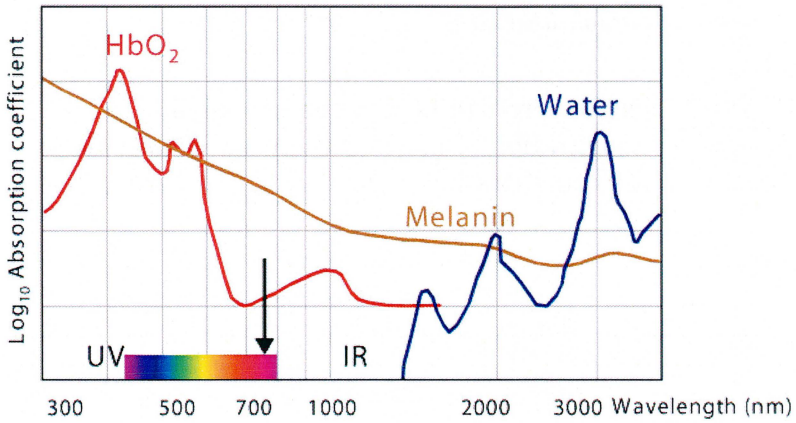

Figure 2.16: *The absorption in human tissue due to hemoglobin (HbO_2), melanin, and water. The tissue optical window ranges between approximately 600 nm and 1400 nm where light can penetrate human tissue without being substantially absorbed by the HbO_2 or water. The arrow indicates the location of the wavelength for the A band of molecular oxygen [21].*

Chapter 3

Equipment

There were two different absorption spectroscopy set-ups sent to Ecuador; one studying rubidium gas and one using the GASMAS technique. The set-ups consist of mechanical, optical, and electronical parts. Many of these parts are shared between the set-ups. This results in that both set-ups cannot be used at the same time.

The rubidium set-up is a good and simple example of absorption spectroscopy and is therefore often used in laboratory exercises in absorption spectroscopy. The essential parts are a diode laser, a glass cell containing rubidium gas, and a photo detector. The GASMAS system, see Fig. 2.12, is more complex and uses modulation techniques, hence it also needs a modulation generator and a lock-in amplifier. Since it handles smaller signals, it also needs a photomultiplier tube as a detector.

3.1 Diode lasers

In the GASMAS set-up, a 5 mW commercial diode laser from Roithner LaserTechnik (RLT7605MG) is used. These diode lasers lase nominally at around 760 nm. They are commercially used for laser printers [22] and thus, the supply is good and the diode lasers are relatively cheap. The diode lasers used in the GASMAS project cost around $100 each [9].

The diode laser used for the rubidium set-up has to be able to scan either the D_1 line at 794.7 nm or the D_2 line at 780.2 nm, see Fig. 4.2 [23]. The diode lasers tested and used in the Quito set-up only range over the D_1 line.

The diode lasers are physically attached to a laser head (Thorlabs TCLDM9). This laser head also contains a TE cooler element which either cools or heats the diode laser to the constantly monitored temperature given by the temperature controller [24].

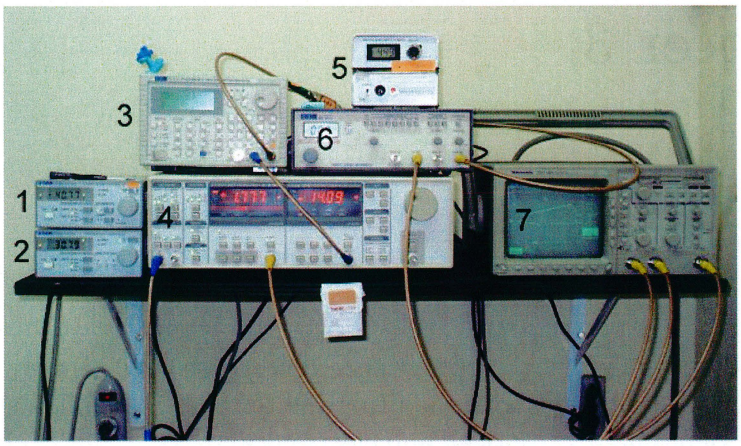

Figure 3.1: *The electronical equipment used for GASMAS; 1. Laser driver, 2. Temperature controller, 3. Modulation generator, 4. Lock-in amplifier, 5. PMT voltage supply, 6. Ramp generator, 7. Oscilloscope.*

3.2 Laser controllers

Two essential parts of the equipment to control the diode laser are the laser driver (ThorLabs LDC202) and the temperature controller (ThorLabs TED200). The laser driver provides the current needed to drive and tune the diode laser. The temperature controller is used to determine the temperature and then steadily keep the temperature at this given limit. This limit is important since a small change in temperature will shift the wavelength of the diode laser. The controller is able to regulate the diode laser temperature from -40°C to +150°C [25]. However, for practical reasons in the experiments with our set-up, the temperature was limited to values between 15°C and 55°C. Outside of these limits, the temperature regulation mechanism for reaching the extreme temperatures was too slow to be functional. Normally, it is advised not to go below 10°C or above 50°C because of risk for water condensation or thermal degradation [8].

3.3 Function generators

Two function generators are used; one to ramp the current to the diode laser and another one for the modulation frequency. In this report they are defined as *the ramp generator* and *the modulation generator* in order to differentiate between them.

The ramp generator (Thurlby Thandar TG215) is used to sweep the injection current with a saw-tooth signal sent to the diode laser. The frequency limit of the generator, for the set-ups used, depends on the lock-in amplifier and the oscilloscope see Sect. 6.2.1.

The modulation generator (Thurlby Thandar TG1010) is used to produce the high frequency modulation signal which is added to the slower ramp, see Fig. 2.10. It provides the reference signal for the lock-in detection. The upper frequency limit is set by the frequency range of the reference channel in the lock-in amplifier. The modulation frequency cannot be higher than half the reference channel frequency limit, since the second harmonic, $2f$, of the modulation signal is studied. The lock-in amplifier used has an upper reference channel frequency of 102 kHz [26]. Therefore, a modulation frequency higher than 51 kHz cannot be used when the second harmonic is studied.

The two signals from the generators are added. This is done by a *power splitter* (Mini-circuits ZFRSC-2050). Depending on how the device is used it can either take one signal and make two exact copies of it, or add two signals into one. However, using the device in this last manner, the amplitudes of the input-signals are halved.

3.4 Detectors

Because of the various needs of the two set-ups, two different detectors are used; a solid-state photo detector and a photomultiplier tube (PMT), both creating a current proportional to the detected light. The PMT is a more sensitive detector and has a larger detection area, which is preferable when absorption in scattering materials is studied. Each detector could be used for both set-ups, but normally the PMT is preferred for the GASMAS set-up and the photo detector is preferred for the rubidium set-up.

3.4.1 Photo detector

A battery driven photo detector (Thorlabs DET110) is used to detect the laser light in the rubidium set-up and for the process of selecting usable lasers. The photo detector uses a photodiode to create a current proportional to the detected light. The detector can be saturated by a too high intensity of light.

3.4.2 Photomultiplier tube

In the GASMAS set-up, the intensity of the detected light is normally very weak since it is attenuated in a scattering medium. In order to detect this small intensity of light, a photomultiplier tube (Hamamatsu R5070A) is used since it is an extremely sensitive detector. The large detection area is also an advantage since the light is scattered.

A photomultiplier tube consists of a photocathode, an electron collection system, an electron multiplier section (dynodes in a cascade manner), and an anode. When the incoming light hits the photocathode electrons are emitted. If a high voltage is put over the PMT the electrons get directed and accelerated towards the dynodes and the anode. When striking a dynode, the electrons produce secondary electrons, creating a cascade. The anode will receive the electrons and create a current [27]. The high voltage is provided from an external high-voltage supply in the GASMAS set-up.

It is of high importance not to let the signal current from the PMT reach too high values, since this can destroy the device. For the setup, the output current was measured over a resistance and displayed with an oscilloscope. The maximum output current from the PMT is generally 100 μA and it is usually linear up to 10 μA. With a too high current, the PMT gets destroyed because of ohmic heating.

3.5 Lock-in amplifier

The lock-in amplifier used in the GASMAS set-up (Stanford Research Systems SR810) is digital. It has a reference channel frequency that ranges between 1 mHz and 102 kHz [26]. The properties; phase, sensitivity, and time constant, see Sect. 2.4.3, are frequently used to optimize the properties of the lock-in signal.

3.6 Oscilloscope

In order to observe the signals from the detector and lock-in amplifier, an oscilloscope is essential. The set-up uses a 200 MHz digital oscilloscope (Tektronix TDS360) with a GPIB port. This port can be used in order to analyze signals using a computer program, such as LabVIEW.

A 100 MHz analogue oscilloscope (Tektronix 2235) was used in parallel with the digital one for a short period of time. Analogue oscilloscopes are better than digital oscilloscopes at showing fast signals superpositioned on slower signals [28], as is the case when an absorption signal is studied in a ramp. It was discovered that small features in the direct signal, like mode jumps and absorption signals, were easier detected with the analogue oscilloscope.

Chapter 4

Preparations

The two set-ups require diode lasers operating at different wavelengths, according to the absorption wavelength of the target gas. Rubidium has strong absorption lines and hence, they are relatively easy to find. Oxygen absorption lines studied in GASMAS, however, are weaker and need modulation techniques. Because of this inequality, different methods were used to find the absorption lines for the gases.

As described before, there are DFB lasers that can be used in absorption spectroscopy. With these rather expensive lasers one do not have to perform extensive testing of the lasers. One of the key features of the project was low cost, so testing mass-produced diode lasers was the option chosen. It was also important to send lasers to Ecuador that did not need to be tested there. The facilities and equipment at EPN are not as suitable for exploring and finding the correct lasers, as at LTH. Therefore these preparations took place in Sweden. The preparations lasted for about six weeks.

4.1 Finding suitable lasers for oxygen

Molecular oxygen has many rovibrational absorption lines around 760 nm, in the A band, see Fig. 2.13. In order to search and find these lines with a tunable diode laser, the maximum current values for different temperatures first needed to be determined not to destroy the laser. When knowing the current values for which the laser could be operated safely, the search for the molecular oxygen absorption signals could be done.

Determining the maximum currents

The maximum current, I_{max}, and threshold current, I_{th}, had to be determined for different temperatures. The threshold current is the injection current where the diode starts to lase and the maximum current is the injection current that gives the maximum power allowed. Between 10°C and 45°C, I_{max} and the I_{th} were determined for every 5°C increment.

An extrapolation procedure was used to determine the threshold current for each laser, at each setting point. A power meter, placed at about 5 cm distance from the laser, was used to measure the output power of the diode laser. For two arbitrarily output powers, between lasing and the maximum allowed, the injection currents were noted. These results were extrapolated to calculate the threshold current and the maximum current values for each diode laser, see Fig. 4.1.

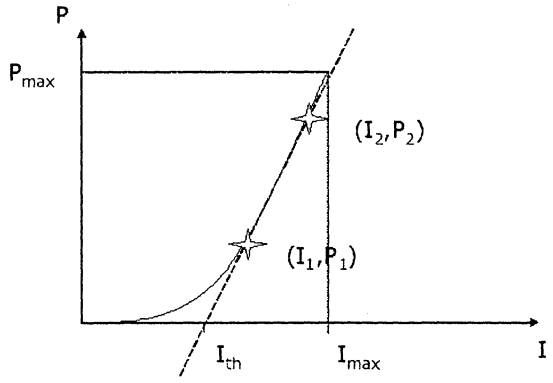

Figure 4.1: *Diagram showing how to calculate I_{max} and I_{th}. The two stars signify two arbitrarily chosen measurement points. An extrapolated line (dotted) from these points is shown together with a line indicating the empirically estimated dependency of the power on the current.*

Signal search

Molecular oxygen absorbs weakly at 760 nm, so to find a laser suitable for oxygen spectroscopy a *long absorption path* was used. This means letting the laser beam pass through as much air as possible ($>$ 10 m) in order to strengthen the absorption signal. The technique was used to find possible absorption signals in the direct signal, see Fig. 2.9.

To investigate these possible absorption signals, a spectrometer was used. The aim was to clarify if the signals were referable to absorption, mode jumps or multi-mode operation. The spectrometer also showed the range, around a certain wavelength, where the diode laser was operating in a single mode. This is a requirement for working around a specific oxygen absorption line.

The investigation was continued using a lock-in amplifier. The settings of the lock-in amplifier were adjusted until a nice absorption signal was obtained. With the help of the lock-in amplifier, additional investigations could be performed to study the absorption signal. On both of the two diode lasers tested, absorption signals were found, but one had nearby mode jumps.

Since oxygen is homogeneously spread throughout the air, a certain distance of air is equal to a certain oxygen concentration. A linear relation procedure was performed to determine that the absorption signal was linearly dependent to the distance of air. By measuring the GMS signal at varying path lengths, a linear relation was determined for the absorption signals obtained with the two lasers tested.

Finally, a wavelength meter was used to determine the wavelength of the laser and thus which line being responsible for the absorption of the light. According to the wavelength meter, the operating wavelength for the best absorption signal found, was 763.31 nm (at 38.08°C at an injection current of 37.4 mA) suggesting that the absorption line observed was P7Q6 [20].

4.2 Finding suitable lasers for rubidium

Rubidium is an alkali metal commonly used in absorption spectroscopy. Its concentration in a sealed-off cell can be investigated by observing the so called D_1 or D_2 lines, see Fig. 4.2. The search for absorption signals, either the D_1 or D_2 line, was done by letting the light from a diode laser pass a 7 cm glass cell containing rubidium gas and observe the output light with a photo detector. The rubidium vapor pressure at room temperature is only 10^{-7} mmHg, but due to the very high transition probability, a strong signal is still expected [4]. Since the exact wavelengths of the absorption lines were known, a wavelength meter was used to measure the wavelength during the signal search to simplify locating the absorption signals.

Most of the diode lasers tested had a wavelength of about 785 nm at 25°C in accordance with the data sheets. Thus, it was necessary to cool the laser

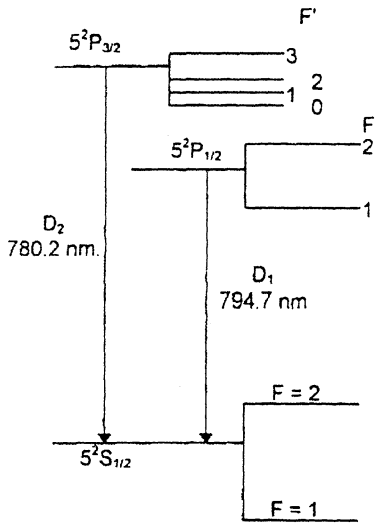

Figure 4.2: *A selection of energy levels for rubidium-87. The transitions called D_1 and D_2 lines are indicated by arrows [23].*

to around 10°C to reach 780.2 nm or heat it to around 45-50°C to reach 794.7 nm. It was, however, not possible to cool the lasers sufficiently to emit light around 780 nm due to restrictions in the temperature controller.

During the investigations, very strong absorption signals were achieved. Thus, neither the lock-in amplifier nor the spectrometer needed to be used. The absorption signals were observed directly as an oscilloscope representation. It was easy to verify that a signal really was an absorption signal, and not a mode jump, simply be removing the rubidium cell and see if the signal disappeared or heating the cell to observe the increase of the signal.

Each laser, of the 18 examined, was tested between approximately 13 °C and 50°C with this method. At an acceptable diode temperature (42 °C) two clear and distinct D_2 absorption lines were found. A few other lasers, operating around 49°C, also detected these absorption lines.

Chapter 5

Technology and knowledge transfer

The task of the project was not only to assemble the equipment but also to collaborate on the local level to build up a knowledge basis around it. Activities were started, aimed to help inspiring students to get involved in the project. Since GASMAS is a rather new technique it was found necessary to introduce it to researchers from other units at EPN, discussing potential applications with them in their own fields of research, and invite them to participate in collaborative experimental studies. During the project a Diploma student, Ms. Yolanda Angulo, was involved full-time. This was an excellent opportunity to share the experience gathered by the authors in Lund during the preparation phase. Ms. Angulo collaborated in all the aspects of the installation and development, learning all the aspects of the set-up.

At institutes such as LTH, the academic and scientific structure is organized in a certain way to foster the education of new students. Graduate students carry on, as part of their duties, the propagation of knowledge on methods and instruments to newcomers. This is an efficient way to keep a basis knowledge at home. However, at places like EPN this does not apply. Undergraduate and Diploma students usually have to help others on their same level to learn. As aid tools for this process, the following activities were worked out:

1. Prepared a scientific poster and posted it together with other written posters about GASMAS on the walls of the department
2. Performed a presentation about absorption spectroscopy and GASMAS

to a general audience

3. Prepared and carried out a laboratory exercise on GASMAS and translated an already existing laboratory exercise instruction for rubidium absorption

4. Wrote a user manual for the set-up

5. Created a website

These five items are described shortly below. We believe that as long as people are made aware of the possibilities, the chances of making productive contacts with other local researchers and of attracting students to get involved, grow significantly.

5.1 Poster

The goal of making a poster, see Appendix B, was to prepare a single-pieced, fully comprehensive document, of high visual impact describing GASMAS, the equipment involved, and some possible applications. Several copies of this poster were made and posted on the campus, along with the invitation to an oral introductory presentation, to stimulate the interest of potential attendees.

5.2 Presentation

In line with our efforts to spread knowledge and inspiration to students and potential collaborate partners at the university an oral presentation was held. This presentation was carried out together with MSc. Linda Persson, from the Lund diode laser spectroscopy group, who was visiting the EPN for about 10 days, supporting the project. The objective of this presentation was to give a detailed and lively introduction to the system. The intention was to present the possibilities of the system to specially invited researchers at the university in order to start a discussion on possible future collaborations. Appendix C shows an Abstract of this presentation.

5.3 Laboratory exercises

Involving many students in the GASMAS activities, including getting hands-on experience with the equipment, was another important objective. By having laboratory exercises, the system will be used by many people and hopefully some students might get interested in continuing to work with the system at the summer practice, Diploma and Master Thesis level.

A laboratory exercise made and frequently used in Sweden for rubidium absorption spectroscopy was translated from Swedish into English and further modified, see Appendix D. A laboratory exercise for understanding the basics of GASMAS was prepared and carried out together with students at EPN, see Appendix E.

5.4 Manual

The experiences from the establishment of the laboratory were discussed and collected in a user manual, see Appendix F. This manual is meant to facilitate the technique and the set-up to future users. It includes a brief theoretical introduction, and a detailed description of the different parts of the set-up at EPN and its operation. Also some basic standard procedures and measurement methods are described. The manual should also be helpful for the trouble-shooting of some possible problems with the equipment. The manual is written with the intention of constant improvement. Hence, a section of the manual was dedicated to instruct these updates.

5.5 Website

A website was set-up in order to have a constant and independent source of information about the project. This website was put on the EPN web server (http://www.epn.edu.ec/Departamentos/fisicaProy.html). It presents the project, gives important contact information, and contains the two laboratory exercise instructions. The website was also constructed in order to be used in the future to present information about ongoing projects etc.

Chapter 6

Assembly

During the preparations in Sweden the entire rubidium set-up and the major part of the GASMAS set-up were assembled and tested. The reason for doing this was not only to test the equipment and to find possible missing parts, but to get hands-on experience on the GASMAS technique and the set-up.

After arriving into Ecuador, there was a two months delay before the equipment could be cleared from the local customs, due to some unexpected problems. In Ecuador the rubidium set-up was mounted first. Because of its simplicity this set-up could be used to test the other parts of the equipment.

After getting the rubidium set-up to function most of the equipment had actually been checked and verified, and the more complicated set-up for GASMAS could be assembled.

6.1 Rubidium set-up

The lasers suitable for rubidium absorption signals found in Sweden turned out not to be so suitable after arriving in Quito. Eventually, the sought absorption signals were found at a ten degrees higher diode temperature than in Sweden and with a significant difference in appearance. The system also showed instability, a signal could suddenly disappear when no variables were changed. After this, the signal took a long time to retrieve and had again shifted in temperature. Parts of these problems were probably due to the laser not working in a single mode. To ascertain that the signal was not a spurious one, the gas cell was either removed to see the disappearance of the absorption feature from the signal, or heated to observe the increase of

the absorption signal. When the temperature is risen the vapor pressure increases, resulting in more rubidium atoms being released from the metal deposit on the cell walls, and hence an enlargement of the absorption signal can be seen. The lock-in amplifier was connected to optimize the detection and to practice working with the lock-in amplifier with a well-defined absorption signal.

The absorption signals showed a W-form, see Fig. 6.1. This was due to the hyperfine structure being visible. The Doppler broadening, which is 0.5 GHz at this wavelength, is smaller than the separation between the transitions, approximately 1 GHz [29], making it possible to see the hyperfine structure.

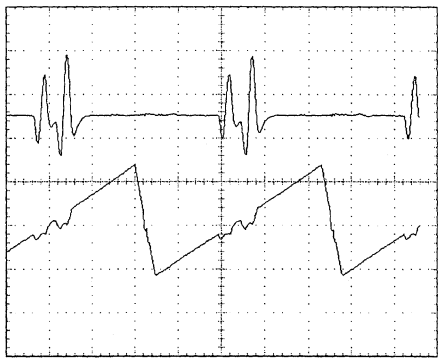

Figure 6.1: *W-shape signals of two absorption lines in rubidium and their corresponding lock-in signal.*

6.2 GASMAS set-up

The same problem with not finding the absorption signals was experienced with the diode lasers for molecular oxygen. Thus, a new search for the absorption signals had to be done. This was once again done with a long absorption path and with the use of a photo detector. The laser output could, however, not be analyzed with a spectrometer or a wavelength meter. This made it hard to know how far the wavelength of the emitted light of the diode laser was from the absorbing wavelengths or how far a mode jump or a multi-mode behavior was from a certain absorption line. After finally finding the absorption signal, an optimization was made on the modulation signal and the lock-in settings.

After the achievement of an optimized lock-in signal, the length dependency was once again tested, this time with a PMT. The output current from the

PMT was measured over an external resistance, 5 kΩ, and analyzed on the oscilloscope. As mentioned before, the current from the PMT should not exceed 10 μA, which corresponds to 50 mV with the external resistance. The direct signal turned out to be very noisy, when the external resistance was used. The noise was found to probably be inherent of the input ports of the lock-in amplifier, and had an amplitude of about 20 mV. Thus, the signal-to-noise ratio was not acceptable. This problem was solved by only using the external resistance initially to determine the maximum current, but while analyzing the signals the external resistance was removed and the internal resistance of the oscilloscope, 1 MΩ, was used.

When measuring the molecular oxygen in a sample it is desirable to avoid measuring ambient oxygen. If the laser beam would go through open air on its way to the sample, the signal would be significantly affected by the oxygen in the air, causing an offset to the absorption signal. In order to avoid this, and for the overall convenience, an optical fiber was used to couple the light from the diode laser to the sample.

When using a sensitive modulation technique, the interference fringes appearing at certain optical interfaces are a problem of great magnitude. Every flat surface reflects some light which can be reflected again from a facing surface, causing periodic intensity variations that overlaps the absorption signals [5, 3]. These fringes show up as a wave-like feature on the lock-in signal, see Fig. 6.2. To minimize the reflections, the fiber ends were polished in angles, but the system still contained fringes after this adjustment. By introducing random vibrations into the whole system, the different reflecting surfaces move and the fringes even out if the signal is averaged.

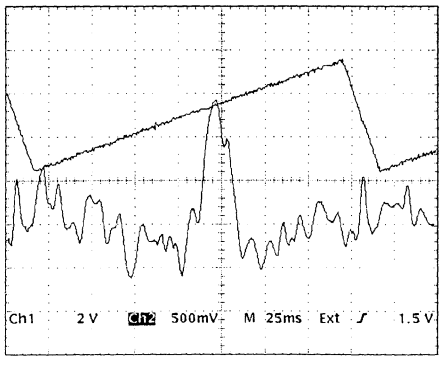

Figure 6.2: *Interference fringes appearing as a wavelike feature on the lock-in signal.*

Initially, the laser beam was focused into the fiber with a lens, but to pre-

vent reflections the lens was removed. This action caused a decrease in the transmission intensity (from 75 % to 50-60 %), but removed the fringes substanstially, together with an offset caused by the air distance.

It was discovered that the ramp signal interfered with the modulation signal in the lock-in amplifier, creating a low-frequency interference. In order to remove this signal a pre-made high-pass filter with a cut-off frequency of 1.6 kHz was put just before the input of the lock-in amplifier.

When the high-pass filter was introduced in the circuit the direct signal almost disappeared. This can be explained by the impedance of the high-pass filter (10 kΩ). Since the oscilloscope has a fixed input impedance of 1 MΩ, a voltage division occurred leaving the oscilloscope with approximately 1 % of the signal. By making two other high-pass filters with the same frequency response but other impedances (100 kΩ and 1 MΩ, respectively), the fraction of the signal to the oscilloscope could be improved.

6.2.1 Optimizing the parameters

The settings of the electronic equipment in general and the function generators in particular are important for a well functioning system. The optimal amplitude and frequency settings for the function generators were systematically investigated by testing different settings from a minimum to a maximum under which the signal could be obtained.

The time constant of the lock-in amplifier was investigated for an optimal setting, which turned out to be 1 ms. Above this value, signals were broadened, and under this value signals were too noisy. This time constant was used for all ramp frequencies.

The amplitude of the ramp selects the observed wavelength range. With a larger amplitude, the signal is less prominent than for smaller amplitude, but more of the surrounding features can be seen. The frequency of the ramp affects the signal if it gets too large, then the signal is smeared out, see Fig. 6.3. This is due to the set time constant on the lock-in amplifier and the sampling rate of the oscilloscope. The time constant averages the signal during this time and hence decides the numbers of samples possible. With a too large time constant or a too high ramp frequency there will be an insufficient amount of samples to provide an accurate signal. The practical frequency limit of the ramp was found to be 20 Hz for the lock-in signal, see Fig. 6.3, but normally ramp frequencies around 5 Hz were used.

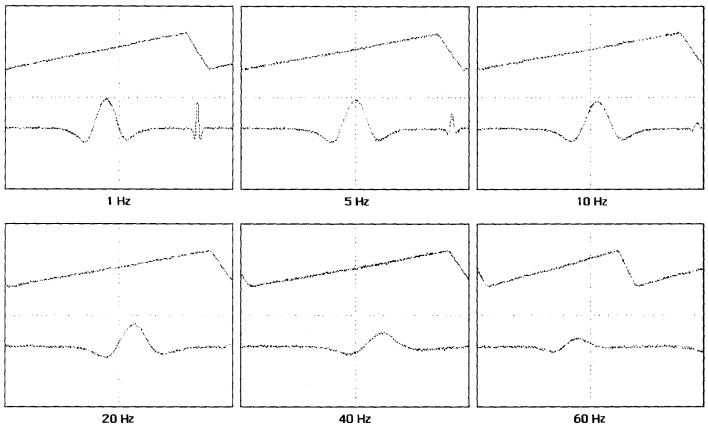

Figure 6.3: *The influence of the frequency and amplitude settings of the ramp generator on the output lock-in signal.*

The modulation amplitude seems to have a relationship with the width of the lock-in signal, see Fig. 6.4. A large modulation amplitude gives a wider absorption signal and vice versa. This is due to fact that the modulated signal observes a wider span. It is also shown in the figure that an increased frequency gives rise to a smaller amplitude of the signal. This might be caused by the electronic components slowing down the transfer function or the modulation frequency being too fast for the diode laser to follow.

The optimal settings of the modulation signal were found to be around 10 kHz in frequency and 60 mV in amplitude. With frequencies under 10 kHz, the signal rapidly got affected by the high-pass filter (with a cut-off frequency of 1.6 kHz) and noise.

6.2.2 Situation specific noise

All unwanted signals in a system that can be detected at the output are referred to as noise. Included are external environmental noise and noise due to certain characteristics of the equipment. Due to the situation of the laboratory at EPN and the specific properties of GASMAS, some particular types of noise were identified. Some of these noise sources were specific for the environment at this very laboratory. As mentioned before, noise types like interference fringes, interference of the ramp, and the noise from the lock-in amplifier were detected and treated, but other types of noise were also discovered.

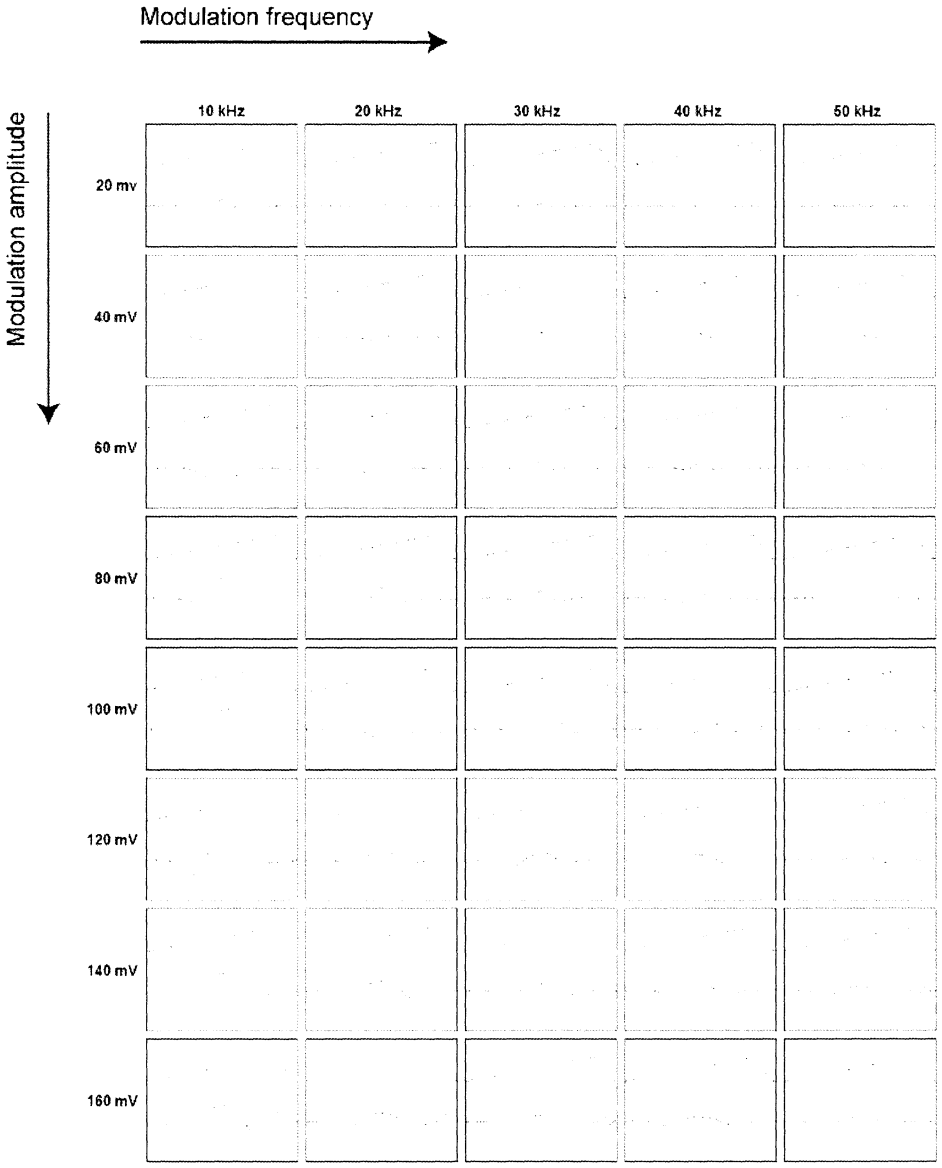

Figure 6.4: *The influence of the frequency- and amplitude settings on the modulation generator on the output lock-in signal.*

Ambient light

Ambient light was detected by the photo detector and caused a noise signal, detectable on the direct signal. Different types of indirect illumination, like sunlight, caused different offsets to the signal. Light from light bulbs or fluorescent lamps caused a 60 Hz noise to the signal and an offset. As expected from the modulation detection theory, this signal did not affect the lock-in signal as can be seen in Fig. 6.5.

The noise from the electrical lights in the direct signal was of course easy to get rid of by turning off the lamps and cover the optical table. Turning off lamps was, however, not always possible because the laboratory was initially shared with an office. Later a wall was built to separate these two rooms, substantially removing this noise source. This wall together with black-painting of the windows also removed most of the offset caused by sunlight.

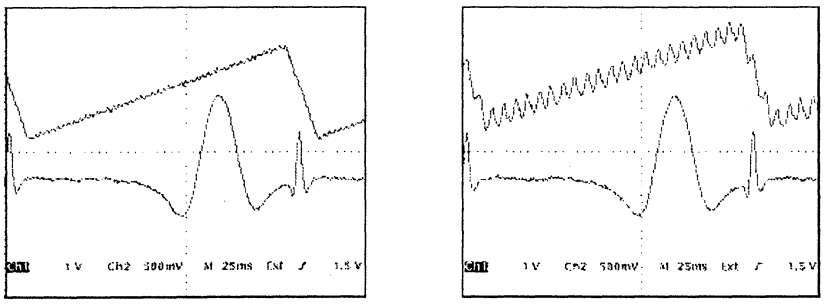

Figure 6.5: *Normal signal (left) and the same signal with a 60 Hz optically coupled noise source (right). The lock-in signal is not affected by the noise.*

Impact vibration

The optics was based on an 60 × 45 cm^2 optical table which was put on a common wooden table. This rather light-weight construction made the set-up easily affected by impulse-like vibrations, propagating from the surroundings into the signals. It was discovered that this was caused by the laser beam alignment moving along with the vibrations and thus, different light intensities were measured at the photo detector. This type of disturbance was somewhat reduced by putting the optical table upon a 10 cm thick bed of soft isolating protection foam.

Bad electrical ground

Having a good electrical ground connection is very important when dealing with scientific equipment. This was a concern at EPN and the set-up was connected to the best possible ground point. A connection to a supposedly better installation in a nearby laboratory with a long cable did not improve the situation, but worsened the quality of the signals. Probably, the cable that connected the two ground points functioned as an antenna and thus was adding high-frequency noise to the system.

6.3 LabVIEW

A computer program was developed using LabVIEW (by National Instruments) to simplify the measurements and make data analysis faster. This program made it possible to transfer the data from the oscilloscope directly into a computer. The functions of the program include the ability to retrieve data from the oscilloscope memory and make automatic calculations. The program calculates the GMS value from the absorption signal and plots the values as well as saves them into a file for further manual investigations. The functions of the program opened up new possibilities for automated and unattended long-time measurements. Measurements that was not possible to perform earlier, could now routinely be accomplished.

There were three major functions of the program, called *Standard addition*, *Single step*, and *Continuous measurement*. The Standard-addition function was made for discrete measurements where the conditions were changed between each measurement. It calculates a GMS value from a signal by making a *zero-level measurement* for each new measurement. A zero-level measurement is defined by us as the measurement of background light. It is measured when the laser is turned off. The Standard-addition function is preferred for measurements that need a high accuracy, such as standard addition. The Single-step function was also made for discrete measurements and works very similarly to the Standard-addition function. The difference is that it does not make a zero-level measurement for each new measurement. Hence, this function is faster but less accurate than the Standard-addition function. The last function, and maybe the most important one, is Continuous measurement. This function is what allows the user to make automated and unattended long-time measurements. The user measures the zero-level through the program, enters the elapsed time of the procedure together with the interval

between each measurement, and starts the measurement. The user interface during run-time can be seen in Fig. 6.6

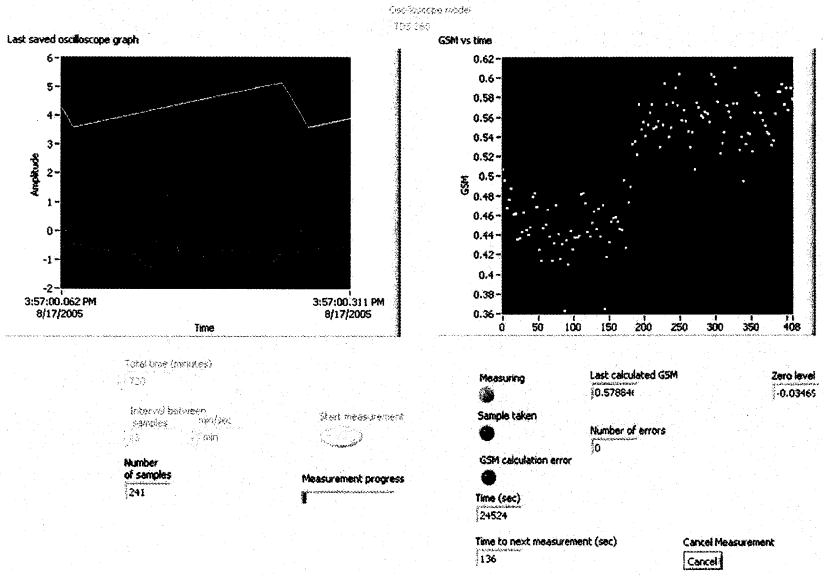

Figure 6.6: *The user interface of the LabVIEW program during run-time for the function Continuous measurement.*

Chapter 7

Experimental work

Experimental work was only performed on the GASMAS set-up. Different experiments were performed to test the functionality and show the possibilities of the system. The first primary test to verify the absorption signals was a lengthy procedure. Before measuring on real samples, different standard addition curves on atmospheric gas were measured to be able to calculate the equivalent mean path length for different samples. With the standard addition curves it was also possible to measure how much molecular oxygen existed intrinsically in the set-up. This was due to small spaces of air in between the optical surfaces in the light path. This resulted in a signal offset that one had to take into account while performing measurements.

Measurements on polystyrene foam slabs were made to study the dependency of the equivalent mean path length on the physical size: width and height, of the scattering medium. Additionally, different types of measurements on fruits, balsa wood, and volcanic rocks were made to evaluate possible applications for the technique. All of these measurements were performed in transmission mode and with a signal averaging 256 recordings per sample. For all measurements the area of detection of the PMT was fitted to the size of the sample. Thus, if the sample did not cover the diameter of the PMT, 25 mm, black paper was used as a mask to block out light.

7.1 Standard addition

As mentioned before, the GASMAS technique estimates the equivalent mean path length by using the standard-addition method. This could be performed

with or without using a sample, comparing only the slopes. The PMT was used as a detector for this method.

When the different slopes are known for different sensitivity settings on the lock-in amplifier, a standard-addition measurement does not need to be done for each measurement.

7.1.1 Sample dependency

The incoming laser light to the PMT was too intense, and thus saturated the PMT, if an attenuator was not used. A standard addition measurement was performed on polystyrene foam, a folded paper, and an optical filter to investigate which sample that was the most suitable attenuator.

Method

The method to determine the standard-addition curves is nothing but a length dependency test. The GMS signal was measured and calculated for different distances of air for different types of samples attenuating the signal.

Results

Table 7.1 shows the different equivalent mean path lengths and the slopes of the standard addition curves obtained for the different samples.

Sample	**Slope (a.u./cm)**	L_{eq} **(cm)**
Polystyrene foam	0.52	30.2
Folded paper	0.68	2.05
Optical filter	0.71	0.57

Table 7.1: *The different standard addition slopes obtained and the calculated equivalent mean path length for three different light-attenuating samples.*

Discussion

Standard addition gave, as expected, different equivalent mean path lengths, depending on which sample being used. The obtained slopes also varied, but should theoretically be the same. Particularly the slope obtained when

using polystyrene foam deviates and this is probably due to the relatively small difference measured upon a large signal and the limit in resolution on the oscilloscope. The folded paper, which is very thin, gives a relatively large equivalent mean path length and this can maybe be explained with the possibly high scattering in the paper and the reflections between the sheets. The equivalent mean path length obtained when using the optical filter can be seen as the internal offset of the system, since the filter provides no additional offset.

7.1.2 Lock-in amplifier sensitivity setting dependency

The slope of the standard addition curve depends on the sensitivity setting of the lock-in amplifier. This mathematical relation was investigated.

Method

Different standard addition curves were measured for different sensitivity settings on the lock-in amplifier. The optical filter was used to attenuate the light to the PMT.

Results

Fig. 7.1 shows the standard addition curves obtained for different sensitivities. The results suggest the following dependency between the slopes of the standard addition curves and the corresponding sensitivity:

$$k_{S1} = \frac{S2}{S1} \cdot k_{S2} \tag{7.1}$$

where k_{S1} is the slope obtained with the sensitivity setting $S1$ and k_{S2} is the slope obtained with the sensitivity setting $S2$.

Discussion

The mathematical relation found between the different sensitivity settings used does not correspond perfectly to the data, but well enough to believe that the mathematical relation is correct. The small discrepancy is thought to be the result of inherent inaccuracies in the measurements.

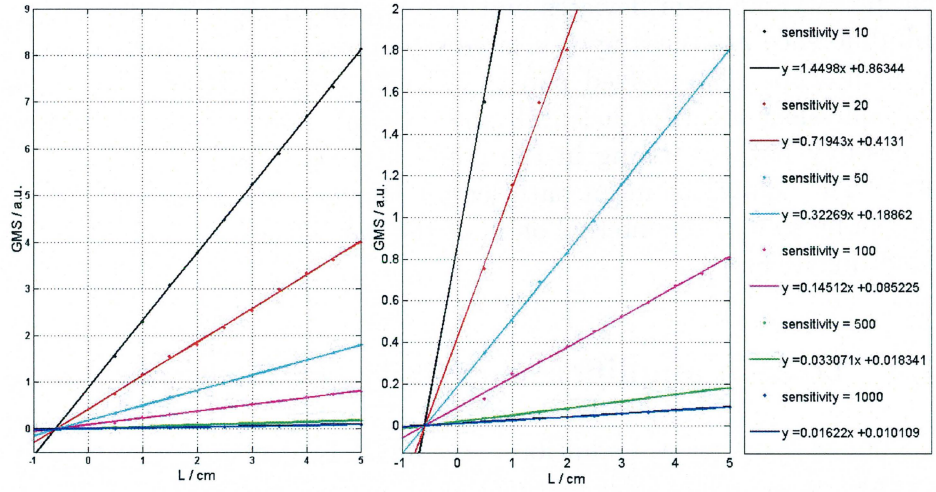

Figure 7.1: *Standard-addition curves for different sensitivity settings on the lock-in amplifier. The left picture shows all the standard addition curves and the right one shows a detailed part of the left curve.*

7.2 Polystyrene foam

Polystyrene foam is an easy material to work with when doing oxygen absorption measurements. The material has high scattering properties and is full of air pockets, both properties give a strong oxygen absorption signal. Thus, the material is useful to investigate the nature of light propagation, such as scattering.

7.2.1 Different width

A measurement on different polystyrene foam slabs with varying widths was performed. This was done to investigate how far the scattering reaches perpendicularly to the incoming beam for a certain thickness of the slab.

Method

To investigate the scattering perpendicular to the laser beam, the oxygen absorption signal was measured for quadratic slabs of 11 mm thick polystyrene foam with different widths, ranging from 0.5 cm to 10 cm in width. The

equivalent mean path length was measured and calculated for every piece. The detector was masked for samples smaller than the detector area.

Results

As can be seen in Fig. 7.2, the equivalent mean path length increases until the piece with a 3 cm width. Thereafter, the equivalent mean path length is stabilized at around 17 cm.

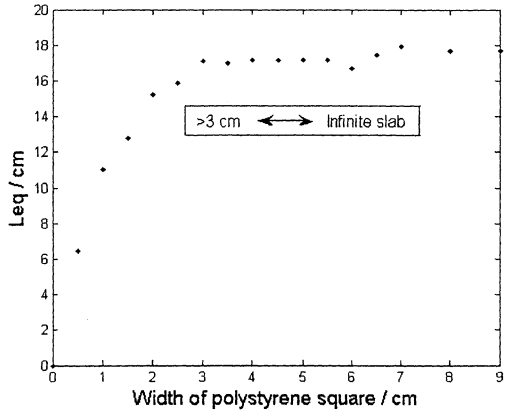

Figure 7.2: *The width dependency of the sample for scattering in polystyrene foam.*

The results indicates that the scattering in a 11 mm thick polystyrene foam sample stretches to approximately 1.5 cm to each side perpendicular to the laser beam.

Discussion

Since the equivalent mean path length is shorter in the smaller slabs, this suggests that the scattered light is prevented by the physical limits of the slab. When the equivalent mean path length values are stabilized, this suggests that the sample could be seen as an infinitely wide slab. A source of error in the measurement is that different detection areas were used.

7.2.2 Different thickness

A measurement was performed on polystyrene foam slabs with different thickness to investigate the effect of thickness of a measured sample.

Method

For this procedure, 7 quadratic 25 $\times$ 25 cm^2 pieces of polystyrene foam were used. The sample thickness was increased by successively putting one on top of the other for each measurement. The equivalent mean path length was calculated for each thickness increment.

Results

In Fig. 7.3, it is indicated how the equivalent mean path length measurements follows a second-degree polynomial fit.

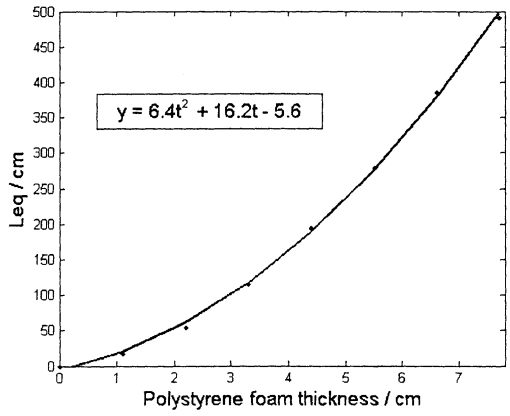

Figure 7.3: *The thickness dependency of the sample for scattering in polystyrene foam. The measurement samples follow the second-degree polynomial fit given in the figure.*

Discussion

The relation between the thickness of a polystyrene foam sample and the equivalent mean path length appears to be a polynome of second-degree

according to the fitted curve. According to earlier investigations this relation should be quadratic [12]. The reason for this discrepancy could be stemming from the large detection area used and the spaces between the polystyrene foam slabs.

7.3 Drying balsa wood

Moisture in wood is a problem in certain applications, e.g. in residential houses. Moisture is also a basic parameter of quality of the wood and is normally estimated as the weight of moisture in the wood compared to the wood. When moisture affects the wood, the air inside the wood is replaced by water [30]. By measuring the decrease of oxygen it is possible to measure the increase of water inside the wood.

7.3.1 Method

A 8×8 cm^2 piece of a 1 cm thick balsa wood was put inside of a bowl of water for 6 hours. The wood piece was removed and the oxygen absorption signal was investigated for about 12 hours as the piece was drying.

7.3.2 Results

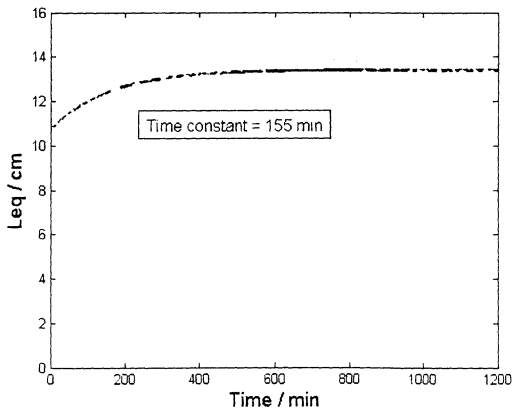

Figure 7.4: *The measurement points made over time while drying a piece of balsa wood. An exponential fit and its time constant are also shown.*

As expected, the oxygen absorption signal increased with time as the water in the wood was replaced with air, see Fig. 7.4. By fitting an exponential curve to the measurement points the time constant could be estimated to 155 min. The piece of wood felt dry when the measurement was finished.

7.3.3 Discussion

The increase in oxygen absorption signal suggests that the water inside the wood is replaced by air. Both the molecular oxygen concentration and the scattering properties probably changed when the piece of wood was drying, giving an increase to the oxygen absorption signal.

A source of error was probably the fact that the zero-level for the normalization was only measured before starting the measurement and not continuously. It has been observed that dry balsa wood allows more light to penetrate than wet balsa wood.

7.4 Fruit and vegetable overview

Ecuador is a country full of different exotic fruits and vegetables providing income to the country through export. Thus, investigating oxygen concentration in fruits is of great importance.

The availability of oxygen affects the ripening process and the quality of the fruit since the gas is a part of the metabolic processes of respiration. The respiration rate of the fruit is proportional to the organic breakdown. So, if the oxygen concentration inside the fruit is decreased, the life time of the fruit is prolonged. However, if the oxygen concentration decreases below a critical level, fermentation starts which initiates a rapid decay of the fruit. Thus, optimizing the concentration of oxygen is of great interest during the postharvest time of the fruit [17].

An investigation was done on several types of fruit and vegetables to test if GASMAS could give some information on their inner content of molecular oxygen and their ability to be tested with the GASMAS technique. This information could be useful not only to give an idea about the limits of the system but also to provide an idea about which fruits and vegetables that can be investigated in the future. The fruits and vegetables chosen are all grown in Ecuador.

Figure 7.5: *The fruits and vegetables tested. Top row, from left: papaya, bananas, tree tomatoes, potato, Hawaiian papaya. Second row: coconut, avocado, passion fruit, physalis, horitos, cassava. Third row: pitaya, apple, guayaba, naranjilla, taxo, granadilla. Bottom row: aloe vera.*

7.4.1 Method

First, different kinds of fruits and vegetables, see Fig. 7.5, were tested to see if useful oxygen absorption signals were obtained. Some of the fruits that gave a molecular oxygen signal were further analyzed which is described in the following sections.

7.4.2 Results

Table 7.2 shows that the majority of the fruit gave a descent or good signal. Exceptions were the coconut, cassava, and avocado which completely blocked out the laser light, making it impossible to determine the oxygen presence in these fruits and vegetables. In the Hawaiian papaya the laser beam penetrated the fruit, but still no absorption signal was obtained.

7.4.3 Discussion

The results show that banana, tree tomato, passion fruit, physalis, horito, apple, naranjilla, taxo, granadilla, and aloe vera all were possible to test

Fruit	L_{eq} (cm)	Thickness (cm)	Signal appearance
Papaya	10	13	Descent
Banana	2.2	3.5	Good
Tree tomato	1.4	5	Good
Potato	1.0	5	Unsatisfying
Hawaiian papaya	-	7	No signal
Coconut	-	10	No signal
Avocado	-	6	No signal
Passion fruit	6.1	5.5	Good
Physalis	0.9	2	Descent
Horito	2.2	2.5	Descent
Cassava	-	6	No signal
Pitaya	1.1	4.5	Unsatisfying
Apple	20	6.5	Good
Guayaba	5.5	5.5	Unsatisfying
Naranjilla	1.5	5.5	Descent
Taxo	3.5	3.5	Descent
Granadilla	23	6.5	Descent
Aloe vera	1.0	2	Good

Table 7.2: *The fruits tested and their corresponding equivalent mean path length (L_{eq}), the thickness of the sample (at the point of measurement to the point of detection) and the appearance of the signal in relation to the other fruits; no signal, unsatisfying, descent, and good. The denotations of the appearance of the signal are the subjective estimate of the authors and is related to the signal-to-noise ratio.*

further. However, some of these fruits only had a descent signal resulting in a larger uncertainty in the GMS value. The GASMAS technique was not at all able to determine the oxygen concentration in coconut, avocado, and cassava since the laser light would not pass these samples. This is probably due to the dense skin of the coconut and cassava and the large and dense kernel of the avocado. It is possible to use the GASMAS technique to investigate papaya, potato and guayaba but the signals are not ideal with respect to signal-to-noise ratio, making possible measurements slightly unreliable. The reason for why the papaya showed a signal, but not the smaller Hawaiian papaya, could not be determined.

It is difficult to evaluate the equivalent mean path length measured on the majority of these fruits and vegetables since they have never been tested before with this technique. However, there has been measurements on apples before, [17, 18], and the value obtained in our experiment is substantially larger. The reason for this could not be determined, but may be related to a difference in the fruits.

7.5 Cutting a papaya

There are two types of papaya available on the markets in Quito. The smaller one is called Hawaiian papaya and the other, larger one, is solely called papaya. The larger papaya is cheaper per kilogram than the Hawaiian. It is common to make juice from the larger papaya but the juice is slightly sour. A common trick to sweeten the papaya is to cut it, either in superficial stripes on the skin or cut the ends off, and leave it for the night making the sour liquid leak out. By doing this, the papaya gets much sweeter.

7.5.1 Method

First, the oxygen absorption signal was measured in a fresh papaya for about 30 minutes. Thereafter long stripes were cut in the papaya, see Fig. 7.6, so that there would be a contact between the pulp and the air. The measurement of the oxygen absorption signal was continued for 12 more hours after making the cuts.

the environment. Thus, the real aim of this experiment was to show the possibilities to measure on the fruit.

7.6.2 Results

Fig. 7.8 indicates a rapid increase in oxygen absorption signal when the banana was cut.

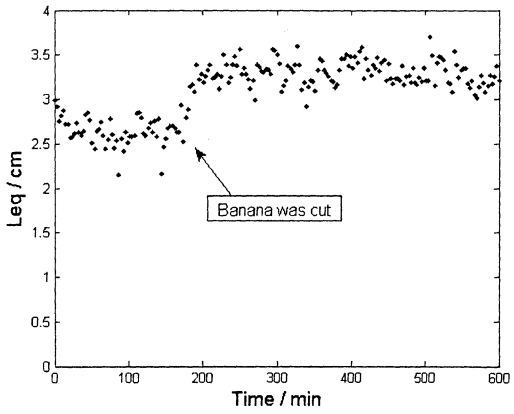

Figure 7.8: *Measurement points showing the equivalent mean path length, L_{eq}, for a banana before and after its ends were cut off.*

7.6.3 Discussion

The oxygen absorption signal increased when the ends were cut off. Even though there might have been a difference in scattering coefficient when the ends were cut off, maybe due to drying, it is suggested that the change in signal is due to a variation in oxygen concentration.

7.7 Peeled apple

Apples are pleasant samples to work with when doing GASMAS measurements. They give a nice absorption signal and are easily manipulated. Studies on gas exchange in apples has been done before, showing the possibilities

to investigate this process using both transmission and backscattering geometry [17, 18].

7.7.1 Method

An apple was measured untreated for about 30 minutes, then approximately 60% of the skin was peeled off while the apple remained under the laser light. The reason for the latter was not to change the measurement point. The apple was measured for additional 10 hours without skin.

7.7.2 Results

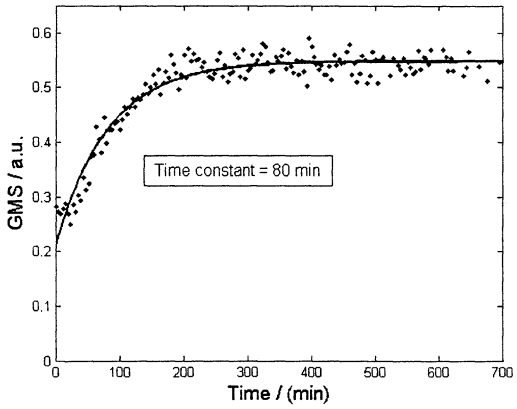

Figure 7.9: *The measurement points and an exponential fitted curve indicating the increase in oxygen absorption signal over time for a peeled apple.*

As can be seen in Fig. 7.9, the oxygen concentration increased when the apple was peeled. The measurement points are fitted with an exponential curve and the time constant was estimated to 80 min.

7.7.3 Discussion

There was a significant increase in GMS signal after the apple was peeled. This suggests that oxygen entered the apple when the skin was peeled off.

Thus, the skin functions as a membrane keeping a certain oxygen concentration in the body of the apple. Similar results have earlier been observed [17, 18].

7.8 Nitrogen exposed tree tomato

Tree tomato is a fruit very similar to the common tomato but slightly different in size and shape. It is also much sweeter and is therefore common in fruit juices in Ecuador. The technique to study gas exchange in fruit by pretreating the fruit by immersion in nitrogen gas has earlier been performed on apples [17], but never on tree-tomatoes.

7.8.1 Method

A ripe tree tomato was put in a glass tank of approximately 25 liter filled with nitrogen at atmospheric pressure. After about 5 hours the tomato was removed from the tank and, instantly, the oxygen absorption signal in the fruit was started to be measured. The objective was to observe the exchange of gases when nitrogen left the sample and oxygen entered.

7.8.2 Results

The results, see Fig. 7.10, indicate an increase in oxygen absorption. The measurement points were fitted with an exponential curve and the time constant was estimated to 25 min.

7.8.3 Discussion

The increase in oxygen absorption signal increased as expected. Since the fruit was not manipulated in any other way than the change of gas environment, it is suggested that the increase in oxygen absorption signal is due to the increase of molecular oxygen in the sample. The skin of the tomato functions as a membrane, providing the fruit with an environment related to the gas environment. When the environment is changed, the gas content inside the fruit changes as well.

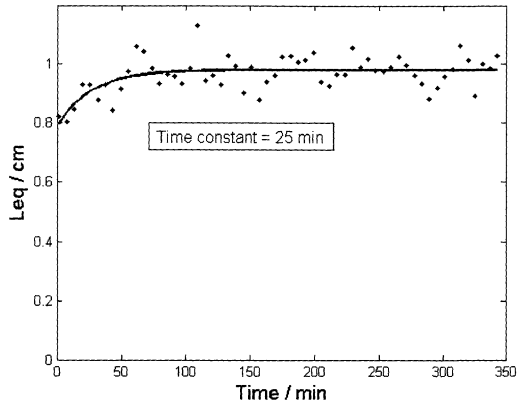

Figure 7.10: *The measurement points and an exponential fitted curve for the measurement of oxygen absorption in a tree tomato over time. Before the measurement, the tree tomato was immersed in nitrogen gas for about 5 hours.*

7.9 Volcanic rock overview

There is a great volcanic activity in Ecuador with volcanoes erupting in the past few years. Thus, understanding the nature of volcanoes is a very important issue for the country of Ecuador and investigating the presence of gas in volcanic rocks might provide important geologic information. In order to give an overview for further investigation, some different types of volcanic rocks were investigated.

7.9.1 Method

The different types of rocks, see Fig. 7.11, were provided by the Department of Geophysics at EPN. They also sliced the samples so that the samples would be geometrically suitable for measurement with GASMAS. The rocks were measured to see if a signal could pass through the rock and the quality of this signal was determined.

7.9.2 Results

Table 7.3 shows that the GASMAS system was not able to measure an oxygen absorption signal in the volcanic rock samples provided. None of the

Chapter 8

Summary and conclusions

There have been four distinct parts involved in this project; preparations, technology transfer, assembly, and experiments.

8.1 Results of the project

8.1.1 Preparations

The preparations took place in Sweden and resulted in the finding of different diode lasers suitable for observing absorption lines for oxygen and rubidium. The diode lasers were later used in Ecuador but different absorption lines were observed due to changes in laser performance. The preparations also allowed for a successful delivery of the equipment from Sweden to Ecuador with the help of ISP in Sweden and Prof. Ayala in Ecuador.

8.1.2 Technology transfer

While waiting for the equipment to arrive and during the entire time spent at EPN, efforts were made to transfer the technology and know-how about the equipment. This was done by holding a presentation, making a poster, creating a website, translating and modifying a laboratory exercise about rubidium absorption spectroscopy, creating and carrying out a laboratory exercise for GASMAS and, finally, creating a manual with the practical knowledge gained by the members of the project during the entire project.

8.1.3 Assembly

After the arrival of the equipment, it was assembled and tested. The rubidium set-up was made functional but the signals found were weak and unreliable. The GASMAS set-up was assembled successfully and tests showed promising enough results to allow for live experiments.

8.1.4 Experimental results

Experiments were made on fruits, balsa wood, and polystyrene foam after verifying the signal and making an extensive standard addition procedure.

Standard addition

Standard-addition procedures were made to investigate the relation between the standard-addition curve slope and the sensitivity setting of the lock-in amplifier. A set of standard-addition curves were measured for six different sensitivity settings and the relation could be calculated. The laser beam needed to be attenuated so three different samples were tested for this purpose; polystyrene foam, a folded paper, and an optical filter. The optical filter proved to be the most suitable attenuator.

Polystyrene foam

Measurements on polystyrene foam have been performed to investigate the behavior of scattering in this material. An investigation was performed showing the influence of physical width of the sample. Another measurement performed was to see the relation between thickness of a sample and the equivalent mean path length. The results showed an effect of limited width of the sample that became negligible after a certain dimension, suggesting that the slab could be seen as infinitively wide. The results obtained between the thickness of the slab and the equivalent mean path length followed a second-degree polynomial fit. However, according to earlier investigations, this relation should be quadratic [12].

Balsa wood

A measurement of drying balsa wood was performed to investigate the supposed increase of oxygen in the wood as it was drying. The result showed an increase in oxygen absorption signal, suggesting that when water vaporized from the wood, oxygen entered.

Fruits

First, measurements were made on several different types of fruits to provide an overview of which fruits that gave good enough signals for performing measurements. Papaya, banana, tree tomato, and apple were further investigated. Measurements over time were made when the skin of the fruits was partially removed. All fruits showed a change of oxygen inside the fruit over time. Apple and banana increased their oxygen absorption signal, while the opposite was observed for the papaya. The reason for this difference might be stemming from an initially different oxygen content in the fruit. The exchange of gases in a fruit was also investigated. This was done by measuring the change of the oxygen absorption signal over time, for a nitrogen exposed tree tomato when placed in air.

Volcanic rocks

Measurements were made on two different types of volcanic rocks, pumice and andesite, using six samples differing in color and thickness. Neither of the rocks gave an oxygen absorption signal. This was probably due to the fact that not enough light could pass through the rocks. Thinner samples might give more promising results but the reason could also be a lack of molecular oxygen in the samples.

8.2 Future work

The laboratory at EPN was successfully assembled and was made fully functional. However, necessary measurements on reproducibility and accuracy were never made. These types of calibrations need to be done to make the laboratory usable for advanced scientific studies.

A validation of the system by comparing the GASMAS system with an already validated equipment should be done. There are facilities at the Department of Food Science at EPN holding equipment for intrusive determination of oxygen content inside matter. Contacts have been established with the department to make this possible. The validation process is an important part in the development of the GASMAS technique and is a challenging task for future workers on GASMAS at EPN.

During the entire project, the aim has been to find solutions suitable for the country of Ecuador. The survey measurements on fruits showed which fruits that were suitable for future studies. Evidentially, we did not test *all* the fruit types in Ecuador. While talking with the potential collaboration partners at the Department of Food Science for example, we got to hear about a root called jicama. This root has interesting sugar properties that might make it possible to produce a sweetener that diabetics can use. Maybe it can also be used to produce a sweetener for people who wants to diet. Hopefully, the GASMAS system at EPN will be a tool in understanding the maturity stages of the jicama root which is a problem at this moment.

The fruits we performed successful measurements on can be further and more profoundly investigated in the future. We have full confidence in that the staff at EPN will find out interesting and exciting experiments to be made. Hopefully, the GASMAS system will help in solving the vast problem of understanding the ripening process occurring while transporting the fruits. This might provide the tools for increasing the possibilities to export the fruits.

The gas content of volcanic rocks can give important and interesting geological information, so the investigation of these rocks will be an interesting objective for the future. A new investigation needs to be done to determine the thickness needed to be able to let enough laser light through the sample to allow a gas measurement. Oxygen is not the most important gas in these contexts so investigations to determine the concentration of SO_2 in volcanic rocks should be a future challenge. Our hope is that the cooperation with the Department of Geophysics will continue and bear fruit in the future.

Many different types of investigation have been thought of throughout the project and many of them were never realized due to priorities on other fields. Hopefully, these ideas will be investigated further in the future.

One of these ideas was to investigate wine bottles. The cork of wine bottles helps the wine to keep a slow and steady exchange of oxygen with the environment, much like the skin of the fruits investigated. Some wines are

held for decades to get the perfect taste and aroma. Maybe the GASMAS technique could be used to determine how the wine is doing during this process. Perhaps the oxygen within the wine or within the air gap could provide interesting information about the status of the wine.

Acknowledgments

First of all we would like to thank Prof. Sune Svanberg who made this project possible. His great enthusiasm for physics has inspired us, his knowledge about the field has helped us, and his friendliness towards us has been greatly appreciated by us.

Linda Persson has been our practical supervisor who always took time to answer our numerous questions and inspire us when we felt down. She has been our friend and mentor, providing us with tips and enthusiasm, throughout the entire project. Special thank to your visit to Quito, where your presence gave new inspiration to a project that sometimes felt impossible.

Prof. Edy Ayala and Dr. César Costa both have been very helpful. Their help extended far beyond their professional duties making us feel very welcome to EPN and the country of Ecuador. Without Prof. Ayala, the equipment would still be at the Ecuatorian customs. Thank you Dr. César Costa for your friendly welcoming and your help with corrections of the report. Also thanks to Christian Santa Cruz who helped us with many practical issues and questions.

A very special thanks goes to Yolanda Angulo who was with us every day during the project in Quito. Her questions made us stay on our toes, her help in the lab (and with the Spanish) was most welcome, and her presence always cheerful.

Mats Andersson and Mikael Sjöholm helped us many times in Sweden. Mats was also very generous with his knowledge about LabVIEW and electronics. He made the task of making a LabView program possible to handle by creating a start program for us and then kept on helping us with problems occurring during the development.

Thanks to our Ghanaian friend Benjamin Anderson who was always very eager to help us while we where doing our preparations in Sweden. We wish you good luck on the project of assembling your own GASMAS setup in

Ghana.

We would also like to thank ISP for not only sponsoring the whole project itself but also our plane tickets to Ecuador. Thank you Lennart Hasselgren and AnnaKarin Norling also for all administrative help.

We would like to thank Äpplets Hus at Kiviks Musteri for a scholarship. We hope you will have use for the GASMAS technology in the future.

Our thanks also goes to Mats Lundqvist for helping us getting started with Latex (the program this report is written in) and Olle Carlsson at ThorLabs, bringing the words Product Support to a new dimension. We also thank Åke Bergquist for preparing the equipment for the Ecuatorian line voltage system and our Spanish teachers with whose help we could actually manage to speak Spanish in the end.

Last, but not least we would like to thank family, friends and our beloved ones; Vannesa and Magnus. Thank you for understanding the need of working far away and long hours. A special thanks to Åke, the father of Märta, who with his visit to Quito shared different ideas and guidance.

Bibliography

[1] M. Sjöholm, G. Somesfalean, J. Alnis, S. Andersson-Engels, and S. Svanberg: Analysis of gas dispersed in scattering media. Optics Letters **26**, 16-18 (2001)

[2] S. Svanberg: *Laser spectroscopy in development, EPN.* Europhysics News (2001)

[3] F. L. Pedrotti, S. J. Pedrotti: Introduction to Optics, 2nd. ed. (Prentice hall, New Jersey 1993)

[4] S. Svanberg: *Atomic and Molecular Spectroscopy - Basic Aspects and Practical Applications*, 2nd. ed. (Springer-Verlag, Berlin Heidelberg 1992)

[5] G. Somesfalean: *PhD Thesis, Environmental Monitoring using Diode-Laser-Based Spectroscopic Techniques*, (Lund Reports on Atomic Physics, LRAP-329 2004)

[6] J. Alnis, B. Anderson, M. Sjöholm, G. Somesfalean, and S. Svanberg: Laser spectroscopy of free molecular oxygen dispersed in wood materials. Applied Physics **B77**, 691-695 (2003)

[7] O. Svelto: *Principles of Lasers*, 4th. ed. (Kluwer Academic / Plenum Press, New York 1998)

[8] U. Gustafsson: *PhD Thesis, Diode Laser Spectroscopy in Extended Wavelength Ranges*, (Lund Reports on Atomic Physics, LRAP-253 2000)

[9] Roithner LaserTechnik Price List, sep 2005. Available at http://www.roithner-laser.com/All_Datasheets/Pricelists/

[10] DFB-Laser diodes, nanoplus GmbH, sep 2005. Available at http://www.nanoplus.com/content/view/23/61/DFB-Laser_diodes.html

[11] An overview of laser diode characteristics, sep 2005. Available at http://www.ilxlightwave.com/appnotes/overview_laser_diode _characteristics.pdf

[12] G. Somesfalean, M. Sjöholm, J. Alnis, C. af Klinteberg, S. Andersson-Engels, and S. Svanberg: Concentration measurement of gas embedded in scattering media by employing absorption and time-resolved laser spectroscopy. Applied Optics **41**, 3538-3544 (2002)

[13] U. Gustafsson, G. Somesfalean, J. Alnis, and S. Svanberg: Frequency-modulation spectroscopy with blue diode lasers. Applied Optics **39**, 3774-3780 (2000)

[14] P. Horowitz, W. Hill: *The Art of Electronics*, 2nd. ed. (Cambridge University Press, Cambridge 1989)

[15] M. Sjöholm: *Diploma Thesis, Development of a laser spectroscopic technique for gas in scattering media*, (Lund Reports on Atomic Physics, LRAP-271 2001)

[16] P. Kluczynski, J. Gustafsson, Å. M. Lindberg, O. Axner: Wavelength modulation absorption spectroscopy - an extensive scrutiny of the generation of signals. Spectrochimica Acta **B56**, 1277-1354 (2001)

[17] L. Persson, H. Gao, M. Sjöholm, S. Svanberg: Diode laser absorption spectroscopy for studies of gas exchange in fruits. Optical and Laser Engineering, in press (2005)

[18] L. Persson, B. Anderson, M. Andersson, M. Sjöholm, and S. Svanberg: Studies of gas exchange in fruits using laser spectroscopic techniques. Frutic05, Montpellier (2005)

[19] L. Persson, K. Svanberg, and S. Svanberg: On the potential of human sinus cavity diagnostics using diode laser gas spectroscopy. Applied Physics **B**, in press (2005)

[20] The HITRAN database, sep 2005. Available at http://cfa-www.harvard.edu/HITRAN/

[21] Modified from: J-L. Boulnis: Photophysical processes in recent medical laser developtments, a review. Lasers in Medical Science **1**, 47-66 (1986)

[22] Laser Applications, sep 2005. Available at http://hyperphysics.phy-astr.gsu.edu/hbase/optmod/lasapp2.html.

[23] A.V. Otieno, B.M.J. Muthoka: Diode laser absorption spectroscopy for teaching undergraduate physics. Africon **2**, 1247-1252 (1999)

[24] ThorLabs: Operation manual TCLDM9, aug 2004

[25] ThorLabs: Operation Manual Thermoelectric Temperature Controller TED 200, jun 2003

[26] Stanford Research Systems: Operating Manual, Model SR810 DSP Lock-in amplifier. (2000)

[27] W.R. Leo: *Techniques for Nuclear and Particle Physics Experiments*, 2nd. ed. (Springer-Verlag, Berlin Heidelberg 1994)

[28] P. Carlsson, S. Johansson: *Modern Elektronisk Mätteknik*, 1st. ed. (Liber, Eskilstuna 2000)

[29] G. Belin, L. Holmgren, S. Svanberg: Hyperfine interaction, Zeeman and Stark effects for excited states in rubidium. Physica Scripta **13**, 351-362 (1976)

[30] V.P. Negodiaev, E.V. Sypin, E.S. Povernov: The monitoring system of wood moisture and air temperature in the drying cell of wood. 5th International Siberian Workshop and Tutorial **IV**, 225-228 (2004)

Appendix A

Work responsibilities

The project was performed by one student at the LTH Engineering Physics branch, Märta Cassel-Engquist, and one from the Electrical Engineering branch, Christoffer Björkwall. This made marks in the way the work responsibilities were divided. Below follows an approximate division of work for these two project participants.

The preparatory work took place in Sweden and includes preparational experiments and arranging for shipping the equipment.

Administrative work included booking plane tickets, buying fruit samples etc.

Experimental work includes mounting the equipment, searching for and fixing errors, calibrating the equipment, and doing experiments.

Report writing includes everything having to do with producing the written report, such as information searching, picture making and of course, the

Task	**Märta**	**Christoffer**
Preparatory work	50%	50%
Administrative work	50%	50%
Experimental work	60%	40%
Report writing	50%	50%
Technology transfer	50%	50%
LabVIEW programming	0%	100%
Miscellaneous	50%	50%

Table A.1: The distribution of work for the two participants of the project.

actual writing of the report. This post also includes the preparation for the presentation.

Information activities include making the two laboratory exercise instructions, having presentations, making a poster, making a website and writing a user's manual.

LabVIEW programming includes the development of a computer program, using LabVIEW, to be used together with the equipment.

Miscellaneous includes everything not possible to put under the other subjects, such as meetings, study visits, building shelves for the electrical equipment etc.

Table A.1 shows the different parts of the project and the percentage performed for the participants. As can be seen the majority of the parts are performed by both of the authors. However, different aspects of the parts have been done, dependent on the specific backgrounds.

The project was started January 24th and ended September 7th 2005. During this period, there was a break in the hands-on work with the equipment between March 6th and May 12th, since the equipment was held at the customs of Ecuador.

Appendix B

GASMAS poster

GASMAS

GAs in Scattering Media Absorption Spectroscopy

Lund Institute of Technology
Lund University

Märta Cassel-Engquist, Christoffer Björkwall, Linda Persson and Sune Svanberg
Atomic Physics Division, Lund Institute of Technology, P.O. Box 118, SE-221 00 Lund, Sweden. Email: Sune.Svanberg@fysik.lth.se

Edy Ayala and Cesar Costa
Departamento de Fisica, Escuela Politecnica Nacional, Ladron de Guevara, E 11-253 Quito, Ecuador. Email: eayala@server.epn.edu.ec

ESCUELA POLITECNICA NACIONAL

Motivation

GASMAS, GAs in Scattering Media Absorption Spectroscopy, is a novel developed technique for measurements of gas contents inside porous, scattering media such as fruit and the body [1-6]. This leads to a wide range of applications.

The key component in the setup is a diode laser, which makes it small, cheap and easy to handle. These aspects are of importance for commercial use in the future.

So far measurements have only been performed on molecular oxygen. However, by changing the diode laser, and thus the wavelength, it is possible to detect other gases, such as CO_2 and H_2O.

The setup

The fundamental components of the GASMAS setup, and other methods for gas absorption spectroscopy, are a light source, a sample and a detector.

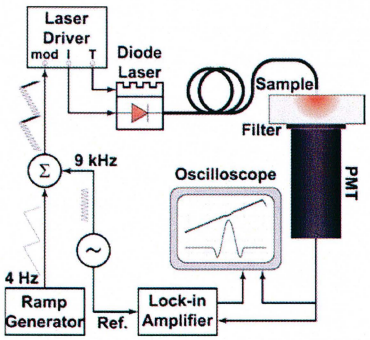

Diode laser – the light source

The diode laser used in the setup depends on the gas of interest. In the current setup a diode laser at 760 nm is used for molecular oxygen studies. The gas content can be estimated by wavelength tuning the laser across the extremely sharp absorption line of the free gas.

Scattering media – the sample

The laser light is guided to the scattering sample by using a fibre. When light has passed the scattering medium, the distance the photon has traveled is always equal or larger than the thickness of the sample, depending on the sample's scattering properties.

PMT – the detector

The photomultiplier is a very sensible detector that measures the light that has passed the scattering media.

Lock in amplifier

The lock in amplifier is a very essential tool to detect and measure very small signals, even though the noise and the background are several orders larger in magnitude.

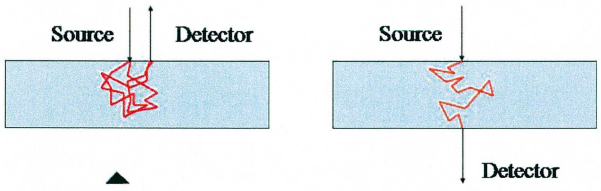

There are two types of detection geometries that can be considered when performing GASMAS measurements; transmission and reflection [5,6].

Current applications

Molecular oxygen concentration measurements inside fruit

Molecular oxygen is a key component in the respiration process of biological tissue, such as apples. A high concentration increases the ripening and too low starts fermentation processes. This makes it very important to be able to control the molecular oxygen concentration inside the biological tissue [4,5].

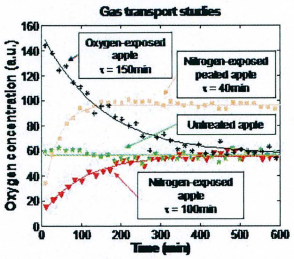

Measurements on respiration rate and oxygen consumption

By measuring the oxygen concentration as a function of time conclusion can be made on gas transport. These results can be helpful to invent a new way of packaging food to last longer [4,5].

Medical applications on sinuses

Very recently measurements have been performed on the frontal and maxillary sinuses by using reflection detection. Normally, to determine if a person has a sinusoidal infection a doctor needs to choose either to perform an expensive CT-scan or just prescribe antibiotics. The results suggest that by measuring the amount of air (indirectly by measuring oxygen) diagnosing the illness can be made cheaper [6].

Potential applications

The body contains many gases and the GASMAS technique can be used to obtain important diagnostic information. A certain gas concentration can be an indicator of an illness or homeostatic imbalance.

Domestic industries like the flower, banana and alpaca industry can have great use of GASMAS technique since they all deal with biologic materials.

Acknowledgments

The GASMAS equipment was donated to the Departamento de Fisica in Escuela Politecnica Nacional, Quito, from the International Science Program, Uppsala, Sweden, in collaboration with the Department of Atomic Physics at Lund University, Sweden.

REFERENCES

1. M. Sjöholm, G.Somesfalean, J. Alnis, S. Andersson-Engels, and S. Svanberg, *Analysis of gas dispersed in scattering media*, Optics Letters 26, 16 (2001)

2. G. Somesfalean, M. Sjöholm, J. Alnis, C. af Klinteberg, S. Andersson-Engels, and S. Svanberg, *Concentration measurement of gas imbedded in scattering media employing time and spatially resolved techniques*, Applied Optics 41, 3538 (2002)

3. J. Alnis, B. Anderson, M. Sjöholm, G. Somesfalean, and S. Svanberg, *Laser spectroscopy of free molecular oxygen dispersed in wood materials*, Applied Physics B 77, 691 (2003)

4. L. Persson, H. Gao, M. Sjöholm, and S. Svanberg, *Diode laser absorption spectroscopy for studies of gas exchange in fruits*, Optics and Lasers Engineering, Accepted (2005)

5. L. Persson, B. Anderson, M. Andersson, M. Sjöholm, *Studies of gas exchange in fruits using laser spectroscopic techniques*, Fruitic05, Submitted (2005)

6. L. Persson, K. Svanberg, and S. Svanberg, *On the potential of human sinus cavity diagnostics using diode laser gas spectroscopy*, Applied Physics B, Submitted (2005)

Appendix C

Presentation abstract

GASMAS
Applied diode laser spectroscopy

Linda Persson, Märta Cassel-Engquist, Christoffer Björkwall, and Sune Svanberg
Atomic Physics Division, Lund Institute of Technology, P.O. Box 118, SE-221 00 Lund, Sweden
e-mail: linda.persson@fysik.lth.se
http://www-atom.fysik.lth.se

Edy Ayala andCesar Costa
Departamento de Fisica, Escuela Politecnica Nacional, Ladron de Guevara, E 11-253 Quito, Ecuador
e-mail: eayala@server.epn.edu.ec

GAs in **S**cattering **M**edia **A**bsorption **S**pectroscopy (GASMAS) is a novel technique developed at Lund Institute of Technology by the research group of Professor Sune Svanberg. This technique deals with non-destructive, *in-situ* measurements of gas inside porous materials such as polymers, ceramics, wood, our body and fruits using narrow-banded radiation from tunable diode lasers. The possibility to measure the gas contained in such materials relies on the fact that solid materials and liquids have broad absorption features with linewidths normally not sharper than 10 nm while free gases typically have a linewidth 10000 times sharper. In the porous materials the radiation is heavily scattered, which results in a not well-defined path length for the light that passes through. The mean path lengths for the light are frequently orders of magnitude longer than the geometrical dimensions of the sample.

The setup is based upon diode laser spectroscopy, with three main components; a light source, sample and detector. Molecular oxygen has so far been studied, by using a diode laser at 760nm. The possibility to use the technique for postharvest monitoring in the fruit industry has been studied by the technique presented. Furthermore, for medicine applications, human trials on the maxillary and frontal sinuses have been preformed for possible use in sinusitis diagnostics, see Fig 1. By changing the diode laser, it is possible to study other gases, such as CO_2 and H_20. The equipment will very soon be available in Quito for research and education purposes.

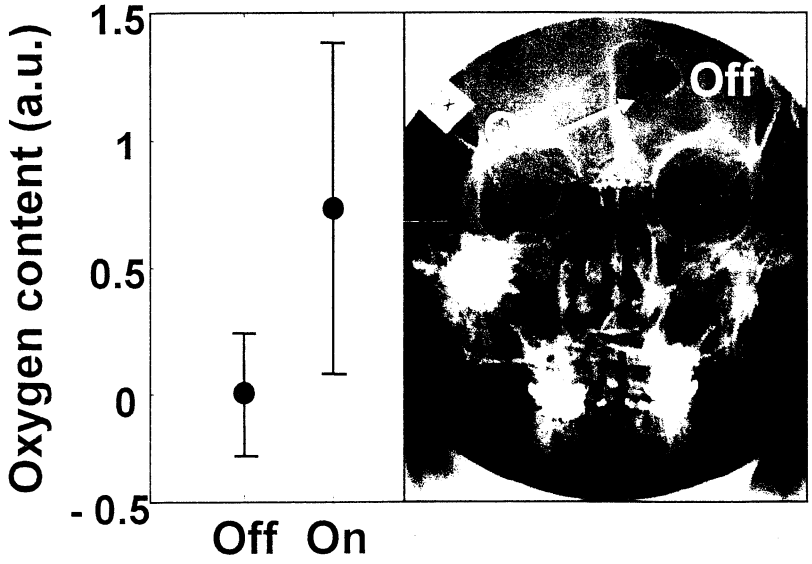

Fig 1. Oxygen concentration measurements of the frontal sinuses.

Appendix D

Rubidium laboratory exercise

Laboratory exercise
Diode laser absorption spectroscopy in atomic rubidium

Originally written at the Department of Physics,
Lund Institute of Technology, Sweden*

Translated from Swedish and modified by
Christoffer Björkwall and Märta Cassel-Engquist
September, 2005

Introduction

The purpose of this laboratory exercise is to give a basic knowledge about diode laser spectroscopy. With the use of laser techniques it is possible to study very detailed structures of the energy levels of atoms. Hyperfine structure, isotopic shifts and Zeeman splittings are examples of detailed structures that can be studied. However, in this lab, we are going to focus on the experimental techniques. Experimental skills of course also include evaluating the results from the measurements. In this laboratory exercise this specifically means understanding the definition of *line width* (for the subject studied and for the light source) and its effect on resolution and measurements of small energy differences.

Regarding the technique of measuring, the goal of this laboratory exercise is to show how to determine gas concentrations by using lasers. Laser techniques can be used to determine everything from the oxygen concentration in a respirator to the air pollutions at a certain level above ground. Dur-

ing this laboratory exercise we will investigate the gas in a rubidium cell by using an absorption signal. When the principle is understood, it is easily comprehended how the absorption path could be a part of a respirator hose or a couple of kilometers of atmosphere.

Preparatory problems

First, read through this laboration manual and do the tasks below thereafter.

1. At room temperature ($20°C$), the vapor pressure of rubidium is about 2×10^{-5} Pa. How many atoms per m^3 does the rubidium cell contain?

2. The distance between the mirrors in a Fabry-Pérot etalon is 10.90 cm. The index of refraction is $n = 1.511$. Determine the *free spectral range* (the distance in frequency between the transmission maxima) of the etalon.

3. A diode laser cavity works in the same way as a Fabry-Pérot interferometer. The free spectral range is 130 GHz and the index of refraction in the resonator is 3.5. How long is the laser?

4. How do you change the frequency of a diode laser? (Practically, there are two ways).

5. Which natural frequency width does the D_2 line of rubidium have if the excited state has a lifetime of 26.0 ns? Which Doppler width does this line have at 20°C and 120°C, respectively?

6. In Fig. 2 there is a Doppler free experimental diode laser recording of a spectrum from the D_2 line of rubidium. Calculate the frequency separations between the ^{87}Rb peaks. Put the ^{87}Rb peak furthest to the left (number 1) as the zero of the frequency scale. (The frequency distance between the 'peaks' in the upper part of the figure is 141 MHz.) Calculate the corresponding frequency separation with the use of Fig. 1 and compare the results with each other. Also determine the *Half Width at Half Maximum* (HWHM) (Δf, measured at half the height) at the highest peak of ^{87}Rb. Compare your result with the natural HWHM (task number 5).

7. Sketch the shape of the spectrum in Fig. 2 if the peaks are Doppler broadened. Use the result from task 5. Is it then possible to see something from the hyperfine structure of the ground state (5s $^2S_{1/2}$) and

the excited state (5p $^2P_{3/2}$), respectively? Estimate the HWHM of the peaks with the help of the separations in Fig. 1 and the Doppler width.

Theory

Hyperfine structure of rubidium

During this laboratory exercise we are going to study the so called D_1 line. Sometimes however, the D_2 line is studied. The original laboration instruction which this instruction is translated from is focused on the D_2 line for example. Thus, the theory and the examples in this instruction will be focused on the D_2 line.

The D_2 line is an historical denotation for the transition between 5s $^2S_{1/2}$ and 5p $^2P_{3/2}$. The denotations D_1 and D_2 do not mean anything. They only refer to that the resonance transitions are appearing in pairs for all alkali atoms. Think about the yellow double line of sodium at 589.6 and 589.0 nm for example. In fact, rubidium has two naturally existing isotopes: ^{85}Rb (73 %), which is stable, and ^{87}Rb (27 %), which, in principle, is radioactive but whose half life is longer than the age of the earth! The resonance (transitions to the ground state from the lowest excited configuration) has the wavelengths

794.7 nm for the D_1 line: 5s $^2S_{1/2}$ - 5p $^2P_{1/2}$
780.2 nm for the D_2 line: 5s $^2S_{1/2}$ - 5p $^2P_{3/2}$

In Fig. 1 it is shown how the hyperfine structure looks for the ground state denoted 5s $^2S_{1/2}$ and the excited state denoted 5p $^2P_{3/2}$ for ^{87}Rb. The energy by the different hyperfine structural levels is denoted by the resulting quantum number F resulting from the coupling between the total angular momentum quantum number of the electronic ($J = 1/2$ or $3/2$) and the nuclear spin I (^{87}Rb has $I = 3/2$). In Fig. 1 the separations in frequency ($\Delta E/h$) between nearby hyperfine structural levels have been marked out. If laser light is to be absorbed, the quantum state F cannot be changed arbitrarily. For allowed transitions the following rules pertain:

$\Delta F = 0, \pm 1$ (F=0 to F= 0 is forbidden)

Thus, we get six spectral lines lying very close to each other in frequency. In Fig. 2 a recording is shown over the six transitions in ^{87}Rb. The numbers at the transitions in Fig. 1 and the peaks in 2 belong together. Consider what will happen when the frequency of the laser is increased. In Fig. 2, even the

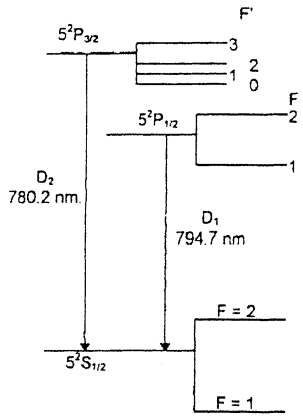

Figure 1: *The energy levels for the rubidium isotope ^{87}Rb. The transitions called D_1 and D_2 are indicated. Transitions between the hyperfine structural levels follow the rule $\Delta F = 0, \pm 1$.*

corresponding transitions at ^{85}Rb (two groups with close lying peaks) are visible.

With rubidium, the separation in frequency between the spectral lines are at most 7 GHz (0.014 nm). It can be seen in both the experimental recording, Fig. 2, and in the energy level diagram, Fig. 1.

Practically, it is not very easy to detect the small differences in wavelengths caused by the hyperfine structure. To better understand the problem, we will briefly discuss line widths.

Line widths

During the laboratory exercise we are using a cell containing a dilute rubidium gas. The laser light getting absorbed by the rubidium gas will be more or less Doppler broadened. *Full Width at Half Maximum* (FWHM) Δf_D for a Doppler broadened spectral line is determined by the temperature of the gas, T, according to

$$\begin{aligned} \Delta f_D &= C \cdot f_0 \sqrt{\frac{T}{M}} \\ C &= 7.16 \times 10^{-7} kg^{1/2} K^{-1/2} kmol^{-1/2} \end{aligned}$$

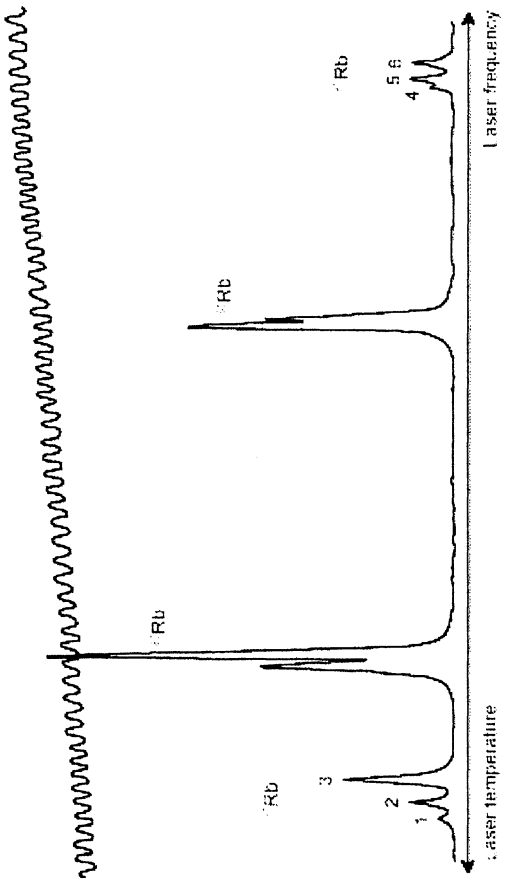

Figure 2: *A laser recording of the D_2 line of rubidium (^{85}Rb and ^{87}Rb) made with a collimated atom beam. In the figure there are also interference fringes from a Fabry-Pérot etalon with a free spectral range of 141 MHz.*

where M is the molecular weight and f_0 the frequency of the transition. Since each line has an individual Doppler profile, small structures are often hidden (in our case the hyperfine structure) because of the lines merging. Thus, it does not help if you have access to a narrow band tunable laser unless you can eliminate the Doppler width.

Even if we successfully and thoroughly eliminate the Doppler width, the spectral lines still have a certain frequency width as a consequence of Heisenberg's uncertainty relation, the so called natural line width. States where the atoms are for a long time (the ground state and meta stable levels), will become very narrow in energy. The frequency width, Δf_N, of an optical transition to the ground state is determined by the lifetime, τ, of the excited state. For transitions to (or from) the ground state, a spectral line will get a FWHM Δf_N determined by

$$\Delta f_N = \frac{1}{2\pi\tau}$$

With a tunable dye laser, with a frequency width of a couple of MHz, it is possible to measure, spectrally, really sharp lines without the bandwidth of the laser broadening the recorded lines. A diode laser, however, has a bandwidth of round 50 MHz which rarely becomes neglible in relation to the natural line width (and the separation between the spectral lines). Thus, we have to pay attention if it is the line profile of the atoms or an instrumental broadening (or a combination of them) that is being observed.

The diode laser

During the laboratory exercise we will be studying ^{87}Rb with the use of a diode laser emitting infrared light at the D_1 line (794.7 nm). A diode laser is shown in Fig. 3 and is an GaAlAs diode laser of the same type as in, e.g., CD players and laser printers. It gives a maximal output of 10 mW, which is enough to be harmful to our eyes (lasers are considered harmful above 0.4 mW). The wavelength 794.7 nm lies just within the limit of the infrared region, and the usual sensibility of the eye is therefore very low. Thus, the light from the laser can seem very weak but still be so intense that it is harmful!). At the laboratory there are safety goggles and an IR card. With the help of the IR card it is possible to localize the IR laser beam. Please, consider the fact that wrist watches and other reflecting parts can cause hazardous reflexes when adjusting the laser beam.

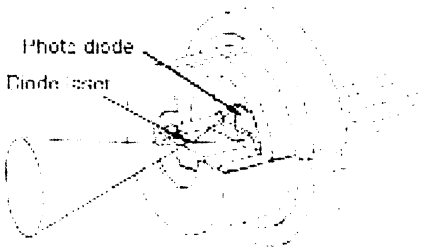

Figure 3: *The diode laser is mounted within a hermetically sealed capsule. The photo diode is used to monitor the laser intensity.*

The laser is of the single-mode type, i.e. it emits light with only one frequency and it has a line width of about 50 MHz. The emission wavelength of the laser (about 794.7 nm) is determined primarily by the band gap in the pn transition. By changing the temperature, the band gap is changed and also the optical path length is changed a bit. Due to the shape of the resonator (the cavity) and the amplification profile the laser sometimes does a jump in frequency (a so called *mode jump*). This means that the wavelength is changed completely, for diode lasers of GaAlAs-type, with about 0.3nm/°C. Between the mode jumps the wavelength is changed 0.06 nm/°C. (or in another words -30 GHz/°C). In Fig. 4 it is shown how the wavelength depends on the temperature.

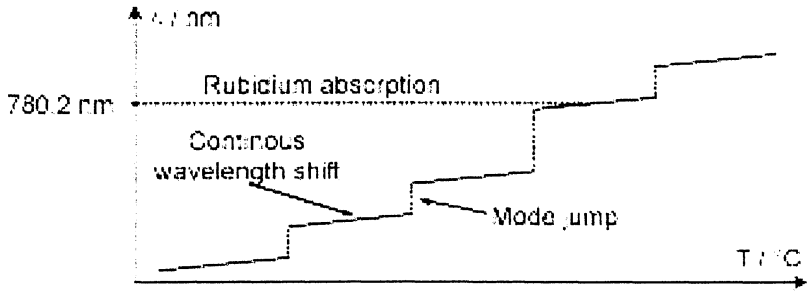

Figure 4: *The emission wavelength of the diode laser is dependent of its temperature. Note the sudden changes in wavelength.*

The light intensity of a diode laser depends on the injection current, Fig. 5. As long as the injection current is small the component functions as a regular light emitting diode (LED). When the injection current exceeds a certain threshold value (denoted I_{th}), light amplification occurs through stimulated emission, i.e. laser action. The injection current needed to generate this

effect varies a bit between lasers. The recommended injection current (I_{op}) is, together with other types of data, given in a data sheet for each diode laser. The laser in this lab can normally be used up to 10 mW, but the life time of the laser will be shortened at this power and if this value is exceeded the laser might be destroyed.

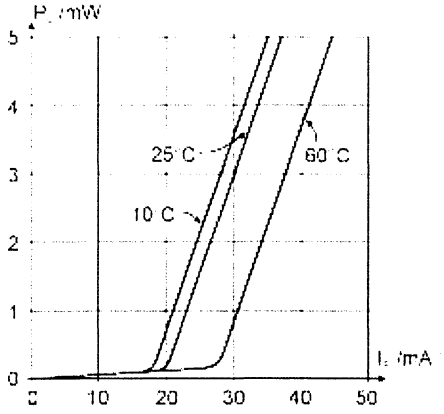

Figure 5: *The output power of the diode laser P_0 as a function of the injection current I_F, for different temperatures.*

The emission wavelength of the laser can also be changed by varying the injection current, which is due to the fact that the temperature is changed locally in the pn junction. We will use this effect to sweep the wavelength of the laser with the help of a function generator.

The function generator can generate a current ramp of which the frequency and slope can be varied. A fast current ramp gives a fast sweep in wavelength, which makes it possible to observe an atomic spectrum in real time with an oscilloscope.

Thus, the wavelength of a diode laser can be altered by varying the temperature of the laser capsule or by varying the injection current. In the laboratory exercise, temperature sweeping is used to coarse tune, and the injection current is used to fine tune the wavelength. The temperature regulator can vary the temperature of the laser between 15°C and 60°C with the help of a Peltier element. This allows for a sweepable range of about 11 nm.

The Fabry-Pérot interferometer

To be able to determine the frequency separation between the spectral lines that the laser light interacts with, we have to generate a frequency scale. A small part of the laser light is sent through a so called Fabry-Pérot etalon. When the frequency of the laser is changed we get a number of interference fringes equally spaced, see Fig. 2. The distance in frequency is called the free spectral range of the Fabry-Pérot interferometer. In the laboratory exercise, an etalon of diffraction index n and the length L is used whose both end surfaces have a highly reflecting layer. The condition for constructive interference is $2nLcos(\theta) = m\lambda$ which reduces to $2nL = m\lambda = mc/f$ for $\theta = 0$. The free spectral range, i.e. the separation in frequency Δf_{fsr} between 2 orders (m and m+1), is then

$$\Delta f_{fsr} = \frac{c}{2nL}$$

The lock-in amplifier

Noise can degrade (or even completely hide) the signal you want to study in a measurement. A signal-to-noise ratio (S/N ratio) is given to describe the situation. If, for example, the S/N ratio is 10 it means that the top of the measured signal is 10 times higher than the average background signal. When the S/N ratio becomes really small it is hard to separate the peaks of the signal from fluctuations of the noise (the background signal). Although, there are measurement methods making it possible to improve the S/N ratio and sometimes even detect signals completely hidden by noise. It is important in some way to reduce the background noise from the measurement for the useful signal to appear.

In the lab a function generator is used. This generator superimposes a modulation frequency upon the injection current. Since the emitted light is directly dependent on the injection current, the light will contain the modulation frequency as well. The signal is then detected phase sensitively at the modulation frequency with the help of a so called *lock-in amplifier*. With lock-in techniques a mixer (also known as multiplier) is used generating the sum- and difference frequencies out of two incoming frequencies.

One in-signal to the lock-in amplifier (the reference signal) is the modulation frequency f_{ref} and the other one is our detector signal f_{det}. Both of the signals are mixed in the lock-in amplifier and the result is $f_{ref} + f_{det}$. Since both of

the signals have the same frequency the result will be a DC-level ($f_{ref} - f_{det}$), which will be amplified, and a high-frequency signal ($f_{ref} + f_{det}$), which will be filtered away. The DC-level depends on the phase relation between the two incoming signals and their amplitudes. It is possible to adjust the phase relation on the lock-in amplifier so that a maximum DC-level can be achieved. The detector signal and reference signals are then in phase with each other. To sum up, it can be said that the lock-in amplifier works like a filter, stops all signals not marked with the modulation frequency f_{ref} and amplifies signals modulated at this frequency.

Procedure

Fig. 6 shows schematically how the equipment will be connected, and what your experimental set-up will look like *after* you performed the tasks 1 to 10.

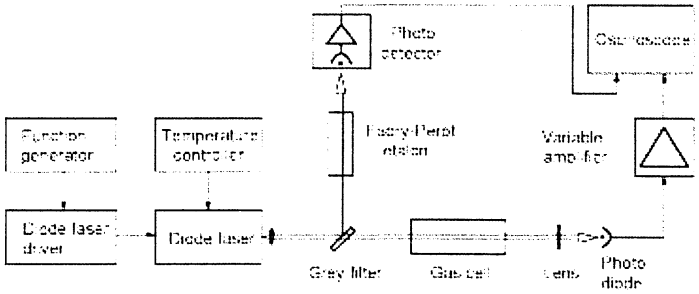

Figure 6: *A schematic of the experimental set-up used in the absorption measurement.*

1. First, get accustomed to the function generator by connecting it to the oscilloscope and make sure you can generate a saw-tooth wave. A suitable ramp frequency is 100 Hz and a suitable voltage amplitude is about 40 mV (peak-to-peak value). When you have set the frequency and amplitude, you connect the generator signal to the diode laser driver modulation input (MOD IN).

   CAUTION! DIODE LASERS ARE EXTREMELY SENSITIVE FOR TRANSIENTS (i.e. electrostatic discharges, cable reflexes etc.). *Never* shut off the current to the function generator or disconnect it from the laser driver unit as long as the diode laser is turned on. Make it a habit to always turn off the injection current (the button at the upper right, **not** the main current button at the lower left) to the diode laser before you make a change in the experimental set-up.

2. Put on the safety goggles. Adjust the injection current to the recommended value I_{op}. The laser is now ready to be used.

3. Focus the laser beam with a lens onto the detector (a photo diode). Connect the detector via the current/voltage-amplifier to the oscilloscope and investigate the detector signal. You will see how the laser intensity varies with the injection current to the diode laser. It is possible that the light intensity becomes so great that the detector becomes saturated (saturation will happen if you really focus the laser beam onto the detector!). Place a grey filter, attenuating the laser intensity 100 times (OD = 2.0), in the beam path.

4. Insert the rubidium cell in the beam path. Be careful with reflexes. The wavelength of the diode laser can now be coarsely tuned by altering the temperature of the entire diode laser capsule. This is done using a Peltier element, in contact with the diode laser. The Peltier element is handled with the help of a temperature controller.

5. Vary the laser temperature ± (10-25)°C around 25°C *at the same time* as you observe the signal on the oscilloscope. The information in the data sheet will give you a hint around what temperature you will find 794.7 nm. The temperature regulator works slowly, have patience and give it time to settle at the temperature you set. If you are lucky you will directly see that the rubidium cell absorbs laser light at a specific wavelength. If not, the absorption lines can be hidden in a mode-jump (see Fig. 4). By changing the injection current a bit the positions of the mode-jumps can be moved. It can take a while even for an experienced experimentalist to find the absorption lines. If you are really unlucky, the entire laser might have to be exchanged.

   If the oscilloscope has problems with triggering, i.e. difficulty giving a stable signal, you can connect the trig output of the function generator (SYNC OUT or AUX OUT) to the external trig input of the oscilloscope.

6. First, control where the level is for 100 % absorption on the oscilloscope screen. Thereafter, put a 50 % grey-filter (OD = 0,3) in front of the detector. Keep the grey-filter with 100 times damping in the beam path. If the signal, i.e. the ramp, on the oscilloscope is damped with 50 % as well, the detector part functions linearly.

7. Investigate what happens with the absorption from rubidium if you place the grey-filter with 100 times damping in the beam path before and after the absorption cell. Try to explain the difference. Make sure

that the absorption is linearly dependent on the laser intensity.

8. Investigate and explain what happens with the absorption signal if you change the injection current to the diode laser and the voltage amplitude on the function generator, respectively. Adjust the injection current and the voltage amplitude so that the largest possible part of the wavelength sweep (for the absorption signal) is being used.

9. Split off laser light from the beam path before the rubidium cell and aim it through the Fabry-Pérot etalon. The laser light should hit a detector (with a built-in amplifier) after the etalon, connected to the oscilloscope. When the reflecting surfaces of the etalon are perpendicular to the laser beam, interference fringes can be observed. The angle of the etalon in relation to the laser beam can be fine tuned with the help of two alignment screws on the etalon holder. The length of the etalon is imprinted on its side. The index of diffraction of the etalon glass is 1,51118 (BK7) and 1,51075 (K8)[1], respectively, at the wavelengths of interest. Thus, it is easy to calculate the separation in frequency between the interference fringes (the free spectral range).

10. Now save the oscilloscope signal from the detector (both from Rb absorption and the Fabry-Pérot fringes) to a floppy disc. This will later be used for an analysis of the spectra. To be able to calculate the absorption, the zero level must be present in the figure, you will obtain this zero level by blocking the laser beam (100 % absorption).

11. Evaluation of the spectrum
    a) Calculate the linewidths (Δf_{abs}).
    b) Calculate the distances between the absorption lines to get the level splittings.
    c) Calculate the absorption, in percent of the light intensity, of the two Rb lines and determine the linear absorption coefficient μ, if we know that $I(x) = I_0 e^{\mu x}$, where x is the path length through the gas and I_0 is the intensity before the gas cell.
    d) Calculate the atom density in the cell. Use the following approximate relation:

$$n = \frac{8\pi\tau\mu_{max}\Delta f_{abs}}{\lambda^2} \cdot \frac{G_1}{G_2}$$

    where μ_{max} is the value of μ at the peak of the absorption profile, and τ is the lifetime for the excited state. The statistical weights can be

[1] These values were used for the Swedish laboratory exercise. They might not apply for this laboratory exercise.

calculated with the results

$$\begin{aligned} \frac{G_1}{G_2} &= \frac{4}{5} \\ \frac{G_1}{G_2} &= \frac{4}{3} \end{aligned}$$

at the strong and the weak absorption signal, respectively.

12. Think about your results. Do your values make sense? Compare with the results of earlier laboratory exercises (ask your laboratory supervisor for these results) and the values you calculated in the preparatory questions (atom density, Doppler width, line width and distance). Comment/explain possible differences. How is the precision and accuracy of the measurement?

13. Rearrange the equipment in the same status as it was when you arrived.

Appendix E

GASMAS laboratory exercise

Laboratory exercise
GASMAS
GAs in Scattering Media Absorption Spectroscopy

Christoffer Björkwall, Märta Cassel-Engquist, Yolanda Angulo
September, 2005

Introduction

This laboratory exercise will introduce a spectroscopic technique called GASMAS. Scattering, absorption, and modulation technique will be introduced and studied. During the laboratory exercise investigations on polystyrene foam and balsa wood will be done. A suitable calibration method, standard addition, will also be introduced.

Preparatory problems

Please read through the entire laboratory instruction, then solve the following preparatory problems.

1. What could happen if the diode laser gets a too high injection current input? If the current output from the PMT gets too high?
2. The current from the PMT is measured over an 5 kΩ external resistance. What should be the maximum voltage measured on the oscilloscope?
3. In Fig. 1 there is an example of an absorption signal and a ramp (PMT current). Calculate the GMS signal. The figure indicates the zero-level

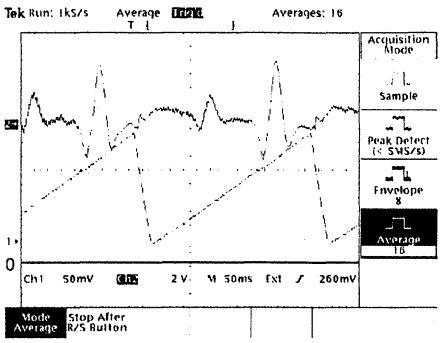

Figure 1: *A mode jump, an absorption signal and the saw-tooth shaped ramp (PMT current).*

with a zero.

4. In figure 16 it is possible to see the signal obtained and the 2nd derivative of an absorption signal and a mode jump. Make a sketch of how you think the 1st derivative would look like for the examples given.

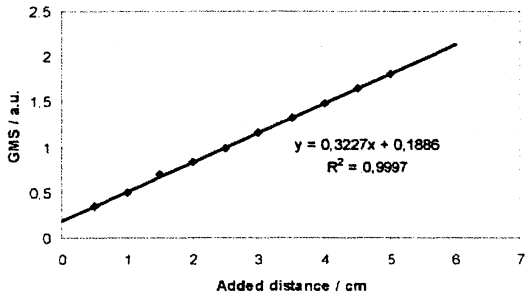

Figure 2: *Measurement plot for a standard addition measurement.*

5. Assume a sample has been studied and data according to Fig. 2 was obtained. What would be the equivalent mean path length of the sample according to this function? Use centimeters.

6. When you perform the standard-addition procedure: What will, theoretically, be the difference between, for example, if you have a sample containing gas or if you have nothing but an optical filter? The equivalent mean path length? The slope of the standard addition curve?

GASMAS

GASMAS, **GA**s in **S**cattering **M**edia **A**bsorption **S**pectroscopy, is a technique that estimates the gas content inside scattering materials such as polystyrene foam, fruits, and the human body. The GASMAS method uses the fact that gases specifically absorbs light with a very sharp and distinct wavelength in comparison with liquid or solid components, such as for example water, which has broad absorption features. The basic components in the GASMAS set-up are a diode laser, a photomultiplier tube, and electronics for the signal detection, including equipment for the use of modulation techniques, see Fig. 3. Currently, GASMAS is focused on measuring molecular oxygen which absorbs light at around 760 nm. Thus, this laboratory exercise is also focused on molecular oxygen.

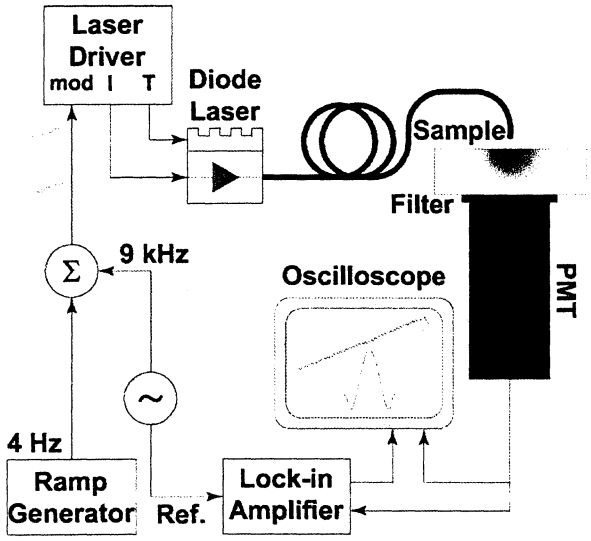

Figure 3: *Figure showing a schematic GASMAS setup.*

Molecular oxygen

Every molecule has, in addition to electronic energy levels, also vibrational and rotational energy levels. During the laboratory exercise an absorption line, resulting from the vibration and rotation energy levels, in the so called *A band* of molecular oxygen will be studied, see Fig. 4. The A band consists of many narrow absorption lines, around 760 nm, with a typical width of GHz in atmospherical pressure.

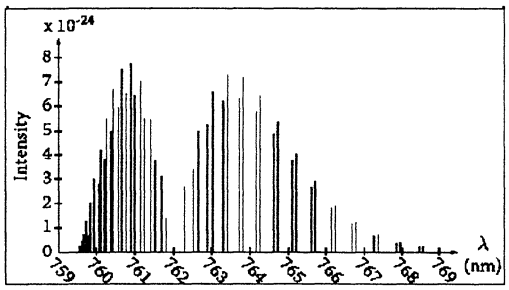

Figure 4: *The absorption lines in the A band of molecular oxygen.*

Diode laser

Diode lasers were introduced about 40 years ago. Since then, they have become the most important type of laser and a daily part of our life, such as in CD players, bar-code readers and printers. They are small and cheap but more important in absorption spectroscopy experiments is that they are possible to tune in wavelength. Fig. 5 shows a diode laser together with a match, pea and a peanut.

Figure 5: *The size of a diode laser in comparison with a match, a green pea and a peanut.*

Diode lasers, or semiconductor lasers, are produced as a compound of different materials. The materials used depend on which wavelength the laser is manufactured to produce. It is today possible to reach wavelengths between 0.4 to 29 μm with different types of diode lasers. The majority of the diode lasers are made of doped materials from group III (e.g. Al, Ga, In) and group V (e.g. N, P, As, Sb) in the periodic system. The first types of lasers produced were the homojunction lasers but they are obsolete today in favor to heterojunction lasers. Homojunction lasers have a more simple construction

than heterojunction laser and will be described as a mean to understand the function of a diode laser.

Homojunction lasers

A homojunction diode laser is created by joining semiconducting materials. One of the materials is *n doped*, has an excess of electrons, and the other one is *p doped* which means it has an excess of positive carriers, called *holes*. When a voltage is applied over the semiconducting material the electrons from the conduction band and holes from the valence band will diffuse through the interface and be able to recombine, see figure 6. As a result, photons will be emitted with the energy corresponding to the band gap.

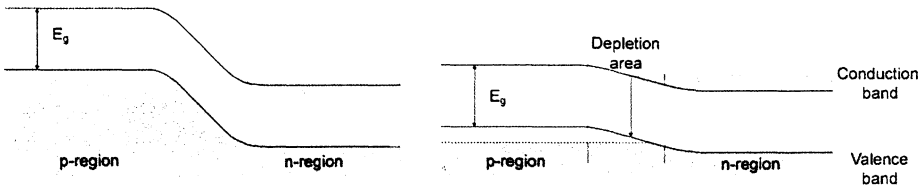

Figure 6: *The band structure of a homojunction diode laser. The left picture is without a voltage put over the junction and the right with an applied voltage.*

The homojunction lasers have a major drawback; they cannot work at room temperature. This is partially due to losses from absorption in the junction.

Heterojunction lasers

Losses from for example absorption of the photons in the cavity, can be reduced in heterostructure diode lasers. Heterojunction lasers are much more used nowadays than homojunction lasers because they can operate at room temperature and do not need to be cooled. The laser used in this laboratory exercise is of the heterojunction type.

The heterojunction lasers have an active layer, which is a semiconductor, sandwiched between the two semiconductor layers with higher band gap energies, as shown in figure 7.

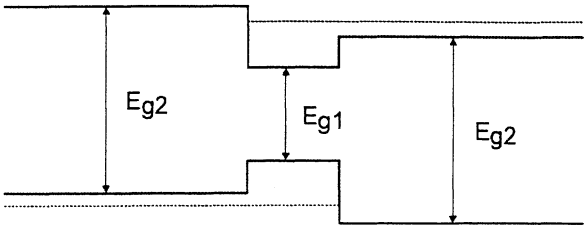

Figure 7: *The band structure of heterojunction diode lasers.*

Laser production

In a diode laser the emitted light will first be spontaneously emitted and with the help of a gain medium and reflectance on the cleaved facets, the photons will be mirrored and a so called cavity is created. As the emitted radiation is able to bounce back and forth this will cause *stimulated emission* and the diode will start to lase, i.e. emit light with the same wavelength and phase, if inverted population is provided.

The wavelength output, and the intensity from a diode laser is dependent on both the temperature and the injection current. At low currents, the output intensity will be low and the diode will only work as a light emitting diode, a LED. When the current exceeds a specific threshold current, I_{th}, the diode laser starts to lase, see figure 8. This threshold current depends on the temperature. By changing the temperature of the diode, the band gap and the optical length change. The wavelength for GaAlAs-type diode lasers changes approximately 0.3 nm/°C. This is the physical reason why diode lasers are possible to tune in wavelength. Hence, the tunability of the diode laser can be done by changing either, or both, the injection current and the temperature. In this laboratory exercise we will try to keep the temperature constant and use the current to sweep the wavelength.

Disadvantages

There are some disadvantages with diode lasers; their output beams are astigmatic, assymetric and divergent. The astigmatism is a result of the fact that the refractive index has a directional dependence. The assymetric and divergent properties of the beam is due to the assymetrical shape of the diode laser (normally rectangular 1 μm $\times$ 3 μm in the active layer). This results in a 10-20° $\times$ 30-50° divergence, see figure 9. The beam, however, resembles a Gaussian profile, which helps to handle this problem.

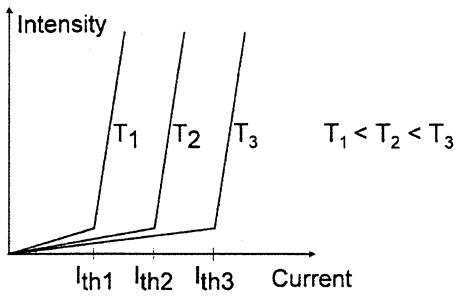

Figure 8: *The output power as a function of the injection current for different temperatures.*

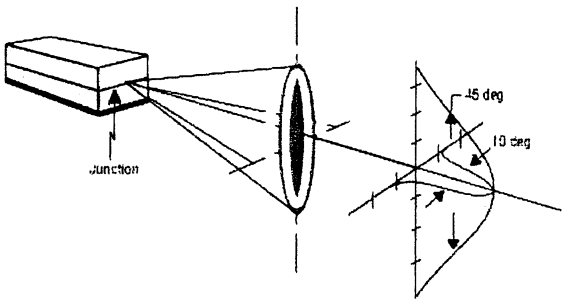

Figure 9: *The divergence features of a diode laser.*

Another more important disadvantage of diode lasers is that they tend to mode jump, i.e. making discrete jumps in wavelength, see figure 10. As with any laser, the output wavelength is the one corresponding to the standing wave in the laser cavity. When the laser is tuned in wavelength the gain curve is shifted, resulting in mode jumps. To fully use the laser properties, it is always important to only have one wavelength in the output from the diode laser, a so called single-mode laser. Multi-mode operation occurs when more than one standing wave in the cavity can lase equally well.

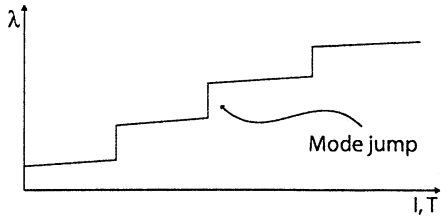

Figure 10: *Diagram showing mode jumps making discrete jumps in wavelength.*

Absorption

Atoms and molecules absorb certain characteristic frequencies or wavelengths. This is an effect of their electronic shell structure and the vibrational and rotational energy levels. If the photon energy, i.e. if the frequency or the wavelength of the light is matching the energy separation of the atom or molecule, it may use the energy and get excited, and the photon is absorbed. Every atom and molecule has a unique set of absorption lines, i.e. its "fingerprint".

Absorption can theoretically be described by the *Beer-Lambert law.* It states that the intensity of the incident light, I_0, attenuates exponentially as the light travels through an absorbing material, see figure 11.

$$I_L(\nu, x) = I_0(\nu)e^{-\sigma(\nu)c \cdot x} \tag{1}$$

The absorption cross section, σ, is the probability of absorption in the unit area per molecule or atom. The concentration of absorbing molecules or atoms per volume unit is c, and x is the length traveled through the medium. The cross section, and thus the transmitted intensity, are both highly frequency dependent, matching the energy level structure.

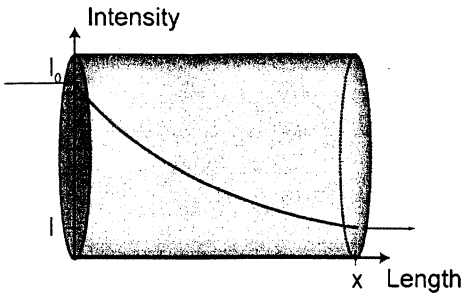

Figure 11: *The absorption of a beam with intensity* I_0

Absorption spectroscopy

An absorption spectroscopy set-up consists of three main parts; a *light source*, a *sample*, and a *detector*. The light is sent through the sample and the output light is detected and measured as shown in figure 12. There are different types of absorption spectroscopies. We will focus on the one used by GASMAS.

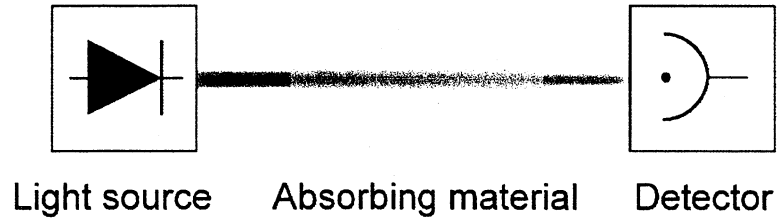

Figure 12: *The three main parts of an absorption spectroscopy set-up for gas samples.*

The properties which can be achieved through absorption spectroscopy is the concentration, temperature and pressure of the sample. The concentration can be calculated from the Beer-Lambert law, equation 1, by measuring I_L and I_0, see figure 13, and knowing the path length and the absorption cross section.

The light source

In GASMAS, a diode laser is used as a light source of the laser light. By letting the injection current have a saw-tooth shape, the wavelength will be repetively swept. The use of diode lasers in absorption measurements is abbreviated TDLAS, which stands for; Tunable Diode Laser Absorption

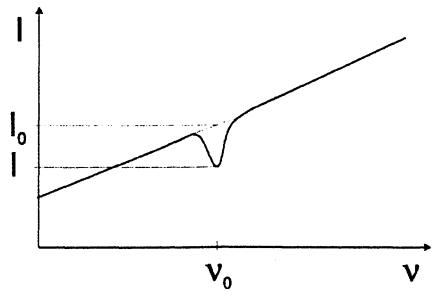

Figure 13: *A sweep in frequency over the absorption line at ν_0. I states the recorded intensity at ν_0 and I_0 the intensity if no absorption would take place.*

Spectroscopy. The diode laser has to be operated with a narrow, single-mode profile to be able to detect the absorption lines.

The sample

In GASMAS the free gas of molecular oxygen inside scattering materials is studied. Scattering occurs when an incident beam interacts with a particle and the reemission of the energy, or parts of it, is in many directions. This effect is a result of the emission from the oscillating electric charges forced by the alternating electrical fields. This scattering process results in the *path length*, the distance the photons have traveled, being greater than the thickness of the sample, see figure 14.

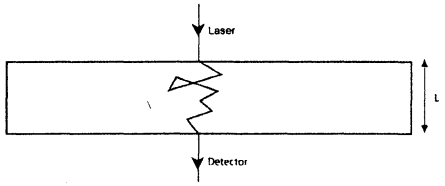

Figure 14: *The distance the light travels in a scattering sample is highly dependent on the scattering of the sample.*

This scattering process complicates the use of Beer-Lambert law, since the actual trajectory is more difficult to correlate with the sample thickness. A unit called *equivalent mean path length*, L_{eq}, can be used to describe the signal. This quantity is obtained by the so called *standard-addition method* discussed further ahead.

The detector

The detector used in GASMAS is a very sensitive instrument, a photomultiplier tube, PMT (Hamamatsu R5070A). The incoming light releases electrons, from a photosensitive material, which are successively and substantially amplified, thus producing a measurable current. Amplification occurs due to the presence of a high voltage difference between the anode and cathode of the PMT, which is supplied by an external high voltage generator. A series of intermediate dynodes divide the full voltage and the amplification is performed in an avalanche through the dynode chain.

It is of high importance not to let the output current from the PMT be too high, since this might destroy the PMT. In order not to exceed the maximum, the output current is measured over a resistance to create a voltage that can be measured with the oscilloscope. The maximum output current from the PMT is 100 μA but it is only linear up to 10 μA.

Modulation

In some applications, the absorption signal is smaller than the surrounding noise. To find these small signals, modulation techniques together with a lock-in amplifier can be used.

When a diode laser scans the wavelength over an absorption line with a ramped signal, a *direct signal*, from the detector is obtained by reading directly the output of the PMT. In some cases, if the absorption is strong enough, it is possible to see the absorption signal in the direct signal, see Fig. 13. In other cases the absorption is small and modulation techniques need to be used. The modulation techniques enable to measure a signal which is only at an order of 10^{-4}–10^{-5} of the direct signal.

Modulation means that a high-frequency sinusoidal signal is added to a carrier signal, e.g. the ramp that scans over an absorption line, see figure 15. The modulation frequency is also sent as a reference to a frequency- and phase-sensitive lock-in amplifier. The output signal from the detector, is filtered by the lock-in amplifier, using the reference frequency, and analyzed. Through modulation, the signal is moved to a detection band at higher frequencies, where the noise level is lower according to noise theory.

Modulation in absorption spectroscopy is also referred to as *derivative spectroscopy*, because the modulation signal gets the form of the derivative if the

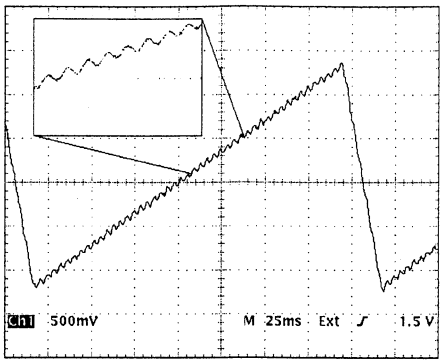

Figure 15: *Ramp with a modulated high frequency sinus function, including a zoom-in on the modulation.*

modulation is small. Figure 16 shows the direct signal for a mode jump and an absorption signal and their resulting lock-in signals.

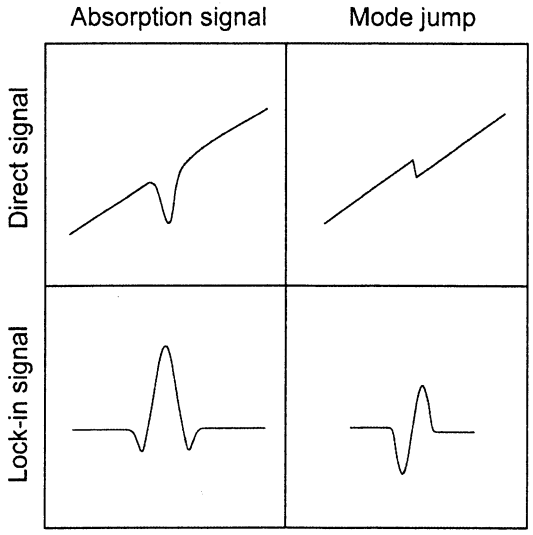

Figure 16: *A comparison between an absorption signal and a mode jump in the direct signal, together with their corresponding lock-in signals. The lock-in signal corresponds to the second derivative of the direct signal.*

Normalization

When dealing with absorption spectroscopy it is of great importance to normalize the signals, in order to be able to compare results. The measured

intensity can vary depending on the sample geometry, the alignment and some other things. In GASMAS, normalization is performed by taking the height of the lock-in signal divided by the intensity of the direct signal at the location of the absorption signature, see figure 17. The normalized signal is referred to as the *GASMAS signal*, and is denoted *GMS*.

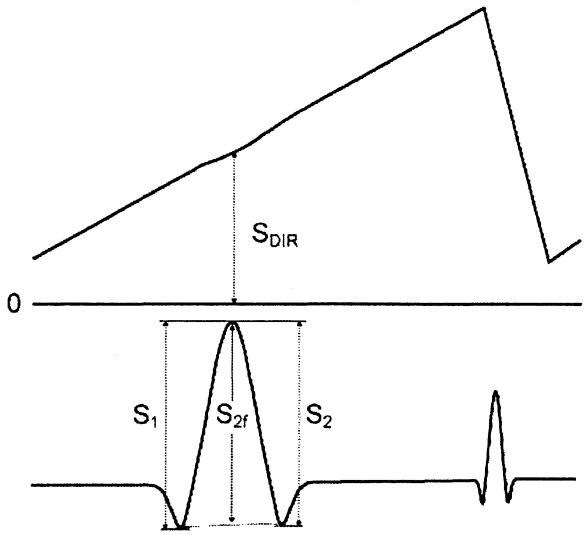

Figure 17: *Diagram showing the normalization measurement points.*

$$S_{2f} = \frac{S_1 + S_2}{2} \tag{2}$$

$$GMS = \frac{S_{2f}}{S_{dir}} \tag{3}$$

Standard addition

There are many ways of estimating gas content. GASMAS uses *standard addition* to determine an equivalent mean path length, which relates the measured signal to that of absorption in free air. In the standard addition procedure, the absorption signal is measured for different distances between the sample and the fiber. With this procedure a calibration line can be drawn and the *equivalent mean path length*, L_{eq}, can be extrapolated, see Fig. 18. The equivalent mean path length defines how much a certain oxygen absorption corresponds to the distance the light would have to travel through air to obtain the same signal. For this reason the equivalent mean path length

can actually be longer, or shorter, than the real thickness of the measured sample.

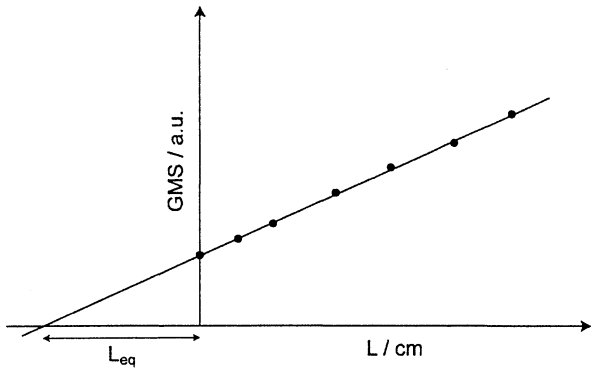

Figure 18: *Several standard addition measurements giving the equivalent mean path length through an extrapolated line.*

The equivalent mean path length, L_{eq}, is dependent on both the concentration of molecular oxygen and the scattering coefficient of the sample. In a highly scattering sample the light will travel a longer distance along more complicated pathways, and hence, there will be larger probability to find molecular oxygen. The real concentration of molecular oxygen in the sample, c_{sm}, can then be related to the concentration in free air, by using L_{eq} according to

$$c_{air} L_{eq} = c_{sm} L_{sm}, \tag{4}$$

where L_{sm} is the actual optical path length traveled by the light inside the scattering sample. One needs, then, to know L_{sm} to determine c_{sm}, or vice versa.

Laboratory exercises

Laser safety considerations

The diode lasers are small and have a relatively low output power, but the laser beam can still be harmful to your eyes. The diode laser used in this lab is of class IIIb, which means that it is potentially dangerous to your eyes by direct incidence, or by diffuse or reflected incidence lasting longer than 10 seconds. The wavelength of the laser is about 760 nm which is a wavelength

where the human eye has low detection ability. But, even if the laser beam seems to be really weak, it might still be powerful! There is an IR card in the lab. With this detection device it is possible to see laser beams at infrared wavelengths.

The diode laser we are using has an output power of about 5 mW. This power is enough to damage the human eye and thus, we need to take certain precautions:

- You should under no circumstances ever look straight into the laser beam. Use the IR card if you need to investigate the path of the laser beam but make sure the reflected light from the card is aimed downwards.
- Take off rings and wristwatches that might reflect the laser light. They can cause hazardous reflections when working with the laser beam.
- Make it into a habit to always turn off the laser when not making experiments.
- There are laser protection goggles (two pairs) in the lab.
- Remember that when working with dimmed light your pupils are larger and more light can come inside. So these recommendations should be considered with attention. Thus, it is advisable to work at a reasonable light level in the laboratory.

Photomultiplier tube

1. Turn off channel 2 on the oscilloscope.
2. Make sure the 5 kΩ external resistance is connected on the input of channel 1.
3. Make sure the voltage from the power supply for the PMT is set to zero. Turn on the laser, and set the temperature and current values if they are not set to the given values.
4. Raise the voltage for the PMT to achieve 10 μA according to your preparatory calculation, but do not let it exceed this value. What this corresponds to on the oscilloscope was calculated in the preparations. A large noise will probably be seen on the screen, depending on amplification etc.

5. Remove the external resistance, without changing anything on the power supply for the PMT voltage. What does the 10 μA current corresponds to now? Remember this value and never let the PMT current exceed this value.

6. Lower the PMT voltage to zero.

Producing a calibration curve for standard addition

Follow the next instructions to generate a standard-addition curve.

1. Put a piece of polystyrene foam on the sample board in between the fiber and the filter to the PMT.

2. Lower the fiber so there is no gap of air between the sample and the fiber, but without deforming the sample.

3. Raise the voltage slowly over the PMT so the current out from the device is 10 μA. Use the value obtained.

4. Turn on channel 2 with the modulation signal.

5. Move the signal with the injection current to the laser so the signal is centered.

6. Press *Harm* on the lock-in amplifier and change it to one. This selects the harmonic studied. The first harmonic corresponds to the first derivative of the direct signal and the second harmonic to the second derivative. Compare with the preparations. Change back to the second harmonic.

7. Change the sensitivity setting on the lock-in amplifier to achieve an optimal lock-in signal, e.g. the highest sensitivity setting achievable without overloading the lock-in amplifier (note that clicking the down arrow will *increase* the sensitivity setting).

8. Measure and normalize to obtain the GMS signal.

9. Raise the fiber 1 cm each time and measure, up to 5 cm. All together 6 measurements.

10. Make a table of GMS vs. height in cm, and from it, make a standard addition curve on the computer and calculate the equivalent mean path length for the sample.

Measurements on polystyrene foam

Different thicknesses

Measure and calculate L_{eq} for different thicknesses of polystyrene foam. What does the dependency look like?

Different widths

You will be given a set of rectangular pieces of polystyrene foam, with different side sizes. Measure and calculate L_{eq} for different widths of polystyrene foam. How do you think the graph would look like? Why do you think you observe a difference in GMS signal for different sizes? Explain.

Measurements on balsa wood

Measure and calculate the L_{eq} for a piece of balsa wood. Consider the actual size of the sample and compare with the measured L_{eq}. Does the actual size correspond to the measured L_{eq}? Why or why not?

Appendix F

Manual

A user's manual named *Manual for the GASMAS set-up at EPN, Quito* was made with the following table of contents:

1. Introduction
2. Background
3. GASMAS
4. Equipment
5. Noise
6. The LabVIEW program
7. GASMAS
8. Procedures
9. Frequently asked questions and common problems
10. Appendix A: Updating this manual
11. Appendix B: Further information